



Railway-induced ground vibrations – a review of vehicle effects

G. Kouroussis, D.P. Connolly & O. Verlinden

To cite this article: G. Kouroussis, D.P. Connolly & O. Verlinden (2014) Railway-induced ground vibrations – a review of vehicle effects, International Journal of Rail Transportation, 2:2, 69-110, DOI: [10.1080/23248378.2014.897791](https://doi.org/10.1080/23248378.2014.897791)

To link to this article: <https://doi.org/10.1080/23248378.2014.897791>



© 2014 The Author(s). Published by Taylor & Francis.



Published online: 25 Apr 2014.



Submit your article to this journal [↗](#)



Article views: 7742



View related articles [↗](#)



View Crossmark data [↗](#)



Citing articles: 76 View citing articles [↗](#)

Railway-induced ground vibrations – a review of vehicle effects

G. Kouroussis^{a*}, D.P. Connolly^b and O. Verlinden^a

^a*Faculty of Engineering, Department of Theoretical Mechanics, Dynamics and Vibrations, Université de Mons – UMONS, Place du Parc 20, B-7000 Mons, Belgium;* ^b*School of the Built Environment, Institute for Infrastructure and Environment, Heriot-Watt University, Edinburgh EH14 4AS, UK*

(Received 5 January 2014; accepted 9 February 2014)

This paper is a review of the effect of vehicle characteristics on ground- and track borne-vibrations from railways. It combines traditional theory with modern thinking and uses a range of numerical analysis and experimental results to provide a broad analysis of the subject area. First, the effect of different train types on vibration propagation is investigated. Then, despite not being the focus of this work, numerical approaches to vibration propagation modelling within the track and soil are briefly touched upon. Next an in-depth discussion is presented related to the evolution of numerical models, with analysis of the suitability of various modelling approaches for analysing vehicle effects. The differences between quasi-static and dynamic characteristics are also discussed with insights into defects such as wheel/rail irregularities. Additionally, as an appendix, a modest database of train types are presented along with detailed information related to their physical attributes. It is hoped that this information may provide assistance to future researchers attempting to simulate railway vehicle vibrations. It is concluded that train type and the contact conditions at the wheel/rail interface can be influential in the generation of vibration. Therefore, where possible, when using numerical approach, the vehicle should be modelled in detail. Additionally, it was found that there are a wide variety of modelling approaches capable of simulating train types effects. If non-linear behaviour needs to be included in the model, then time domain simulations are preferable, however if the system can be assumed linear then frequency domain simulations are suitable due to their reduced computational demand.

Keywords: railway; ground-borne vibrations; track dynamics; railway vibration; critical speed; Hertzian contact; wheel/rail unevenness; multibody systems

1. Introduction

Railways are a solution to traffic congestion and pollution, however one drawback is the problem of noise and vibration. Much energy has been exerted into the goal of reducing vibrations in the vehicle itself while, at the same time, improving passengers comfort. These vibration levels are merely a function of the forces generated by the train vehicle. Therefore when attempting to predict and understand railway vibration, it is imperative that the vehicle characteristics are modelled correctly. This paper seeks to provide a comprehensive review of vehicle modelling procedures and provide a resource for further research.

*Corresponding author. Email: georges.kouroussis@umons.ac.be

Historically, railway lines have been a popular mode of transport for both passengers and goods. Despite this, in recent years there has been increased deployment of new tracks due to the increased competitiveness in comparison to alternative forms of transport. In particular, there has been a surge in tram projects and high-speed rail. This increase in track infrastructure has also boosted track availability on traditional lines, thus facilitating the more efficient movement of freight.

Vibration characteristics vary greatly between tram, freight and high-speed rail locomotives partly because increasing speeds shift the frequency of excitation to a higher spectrum. Additionally, differences between unsprung mass and the typical defects associated with each account for additional variation in vibration generation. Despite this, the vibrations generated from each type have the potential to cause negative environmental effects, particularly to humans and sensitive machinery. Regarding humans, this concerns feelable vibration and structural vibration which causes walls/floors to shake, thus generating indoor noise. This is of particular concern in the absence of airborne noise such as is the case for underground railways. For the sensitive machinery case, structures that rely on the operation of such equipment (e.g. hospitals or manufacturing plants) can be negatively affected by even small levels of vibration.

The generation of vibrations is solely a consequence of the vehicle forces passing from the wheel into the track. These forces arise from the weight of the vehicle and irregularities/discontinuities at the wheel/rail interface and then propagate outwards from the track. The vibration level experienced at all other locations within the track, soil or nearby structures is a function of this force, depending on the natural frequency of each component. Therefore it is imperative that when simulating railway vibration that the vehicle and resulting forces are modelled in a manner that closely approximates the physical problem.

This paper outlines the mechanisms that contribute to the generation of railway vibrations, as well as analysing a variety of modelling approaches for numerical simulation. It also lightly touches on track and soil modelling due to their close dependence on the vehicle excitation. However, it does not discuss external structures due to their weak coupling with vehicle excitation. Furthermore, a variety of modelling parameters are presented with the intention to aid further research into multibody vehicle modelling.

2. Experimental and numerical investigation on railway vibrations – practical considerations

2.1. *Applicability and limitations of experimental investigation*

Physical experiments were the first means researchers used to evaluate the effect of moving rail vehicles. ISO 14837-1 [1] provides a general guidance for measurement methods appropriate for a range of circumstances. More precisely, the location of sensors is defined along a line perpendicular to the track in order to quantify the decrease in amplitude due to a distance from the source. It is also recommended to measure vibration in three directions, defined as x for horizontal (parallel to the track), y horizontal (perpendicular to the track), and z vertical downward.

One of the most popular works cited in literature is the experimental analysis of Degrande and Schillemans [2], which outlined the measurement of free field vibrations and track responses during the passage of several Thalys high-speed trains (HSTs) at speeds varying between 223 and 314 km/h. The uniqueness of this work was twofold: (1) the analysis of a train's speed effect on recorded vibration levels, and (2) the availability of the presented data to other researchers for validation purposes. Other experimental investigations also provided

useful information. For example, the work of Auerch [3] quantifies the declining effect of distance through the depleting relationship with a large database of different technical sources including rail traffic. Madshus and Kaynia [4] used experiments to demonstrate the negative effect of a soft soil site, concluded by a numerical analysis.

Constraints related to the use of measurements include:

- Time and budget constraints generally limit *in-situ* analysis, as detailed in [2]. Furthermore, the complexity of railway-induced ground vibrations is due to the large number of parameters, which influence in the generation and the propagation of ground waves. The investigation of all these parameters is difficult.
- Analysis is often limited to a simple case where only one phenomenon is expected to be emphasized. However, it is very difficult to find an exact site where the objectives of the research correspond to reality (e.g. supercritical phenomena).
- An important aspect, which is neglected, is the signal-to-noise ratio, and more particularly the effect of other external sources (e.g. cars, construction excitation, etc.), which can prevent accurate interpretations of results.
- In some cases, the site for analysis is yet to be created. Preliminary studies and impact surveys are therefore limited to other sites of similar composition.

Despite this, experimental data is interesting because it can be used to establish empirical models and also validate existing or in-development prediction models. It also serves to illustrate essential physical interpretations, as have been found on real lines in the last 20 years.

2.2. *Vibration prediction models*

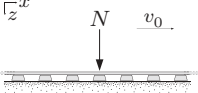
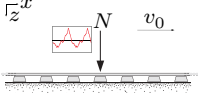
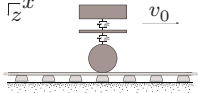
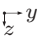
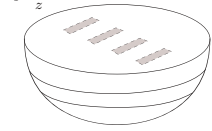
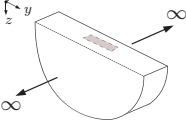
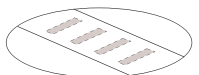

The vibration source and receiver have been studied by many authors who have adopted complementary methodologies both for vehicle and ground wave modelling. Table 1 gives an overview of recent numerical prediction models, which have been classified according to their function of rolling stock and soil modelling. Evidently, the list is non exhaustive, but still succeeds in displaying the evolution of modelling during the last years of development.

The first prediction models [5,6] used a simple point source load to simulate the effect of a moving train. With the intent to further research the vehicle and track interaction exerted by the wheel and rail irregularities, a random part of excitation was quickly completed.

In the renovation of existing lines and the installation of new ones, the assessment of vibrations induced by railway traffic is becoming an important subject of research. To assess the effect of vehicle dynamics on ground motion, calculations must be made of the forces acting on the track/soil subsystem. Most of the existing prediction models, which consider the vehicle as a sequence of axle loads or rigid wheel sets, cannot aid a railway vehicle designer in evaluating significant dynamic modifications brought about in the vehicle itself (excluding the nominal loading per wheel set). To cope with these dynamic effects, some prediction models [7–9] included the vehicle as a multibody system in numerical models, and [10] quantitatively evaluated the effect of a vehicle's structural modification on generated ground vibrations.

Soil modelling often imposes methodology adopted by the vehicle, due to the difficulty of combining two approaches that are fundamentally different. For example, the boundary element method (BEM) is the most popular method because of its innate ability to represent infinite domains and its good computational efficiency when the problem is formulated in the frequency domain [11]. However, the method becomes inconvenient when dealing with complex geometries, and the frequency domain is limited to linear problems. For example, in vehicle dynamics, dynamic simulations are typically

Table 1. Classification of recent railway-induced ground vibration models.

	Constant axle load	Random axle load	Detailed model
Vehicle modelling →			
Soil modelling ↓	Krylov [17,18] Kaynia et al. [19] Sheng et al. [5,20] Degrande and Lombaert [21] Karlström [22] Takemiya and Bian [23] Maldonado et al. [24]	Lu et al. [25] Sheng et al. [26] Lombaert et al. [27]	Datoussaïd et al. [28] Sheng et al. [29] Lai et al. [30] Auersch [31] Xia et al. [32] Lombaert et al. [33]
Analytical solution			
	Paolucci et al. [34] Wang et al. [35] Fujii et al. [36] Yang et al. [37] Vogiatzis [38] Çelebi and Kirtel [39]	Yang et al. [40] Pakbaz et al. [41]	
2D FEM			
	Hall [42] Powrie et al. [43] Anastasopoulos et al. [44] Stupazzini and Paolucci [45]		Gardien and Stuit [46] Ju [47] Zhai et al. [48] Banimahd et al. [49] Wang et al. [50] Kouroussis et al. [8,51] Connolly et al. [52,53] El Kacimi et al. [54] Galvín et al. [9] Costa et al. [7]
3D FEM			
	Sheng et al. [55] Yang et al. [40] François et al. [56] Costa et al. [57] Gao et al. [58]		
2.5D BEM and/or FEM			
	O'Brien and Rizos [59] Andersen and Jones [60] Auersch [61] Chebli et al. [62] Galvín and Domínguez [6]		Galvín et al. [63] Romero et al. [64]
3D BEM (surface)			
	Thornely-Taylor [65] Hussein and Hunt [66] Jones and Hunt [67]		
Alternative approaches			

performed in the time domain (typically if done so with the multibody approach), thus allowing for the simulation of the non-linear behaviour. Alternatives to numerical prediction models exist, based on empirical approaches [12–16]. They are often used during the preliminary design phase.

3. Ground vibration generated due to alternative rolling stocks

The railway industry has existed for many years, and in that time, it has evolved from traditional mechanics to a high-level technological industry. In some countries like China,

the railway still plays a crucial role in transportation. This section provides some interesting elements on the introduction of railway dynamics, and its link with ground vibrations. Additional information can be found in [68–71].

3.1 *A brief history of vehicle evolution*

A train running on a track is a dynamic system and has been in existence since the sixteenth century. It was initially used in mines for the transportation of extracted ore, before being used for the transportation of people as well. The first railway for passengers was opened in North East England in 1825, providing a link between Stockton and Darlington. Ten years later, Belgium became the first country on the mainland of Europe to propose a railway network. Other connections opened, ending with the current web of rail systems as we know them today.

In the beginning of the nineteenth century, the first analyses were conducted on traction using adhesion, which helped resolve the problem of the strength of materials used for the wheels and the rails. The universal adoption of flanged wheels also resolved the problem of navigation on straight or curved lines. This problem is still studied presently; an example of which is the dynamic and stability effect of negative tread conicity for improving steering ability [72]. Contact problems remain an important issue in railway dynamics.

Due to the limitation of vehicles with a rigid wheelbase in curves, bogie systems have been rapidly proposed in rail vehicles in order to prevent hunting motions. Suspensions associated with a bogie are to isolate the car body from excitations upon running contact. Secondary suspension systems are located between the bogie and the car body, and consist of elastomer elements, air spring or metal spring. They are used to bear the car body and allow the bogie to rotate when the rail vehicle experiences bends. Primary suspensions connecting the wheel sets to the bogie frame do so mainly by using coil or rubber springs. The double suspended bogies are not universal: only a single-stage suspension (primary or secondary suspension) is used in carriage trains. The design of a bogie is also associated with ground-borne vibrations. Wilson et al. [73] demonstrated that a proper design of the bogie suspension can significantly reduce the levels of ground vibration. In general, vehicles with soft primary suspension produce lower levels of vibration than vehicles equipped with stiff suspensions [74].

Although other important developments can be analysed, this paper only presents these two concepts, mainly due to their importance in railway dynamics affected by ground vibrations.

3.2. *Vibrations generated by the railway*

According to Alias [75], vehicle dynamics influence the low-frequency range (up to 15 Hz), and are efficiently transmitted to the ground if significant defects in the wheel/rail contact excite the vehicle's natural modes. The upper limit of this low-frequency range is not well defined, and depends on the main vehicle dynamic modes (pitch and bounce modes), on the sprung and unsprung masses, and on their distribution. The high-frequencies (over 150 Hz) constitute another range with rolling noise due to wheel/rail sliding. They cause ground vibrations because the soil efficiently absorbs them (this is known as material and geometrical damping). Between them, the ground vibration spectrum is characterized by the track and soil flexibility, with possible soil resonance due to their

geometry and difference of rigidity of the upper soil layers. Many of these excitation frequencies are approximated in Figure 1, and are based on [76–79].

Figure 2 illustrates three train types according to their network. The trains were classified according to their main excitation mechanisms. HSTs generate ground vibrations that are mainly dependent on quasi-static track deflection, because high-speed lines are typically characterized by very high quality rolling surfaces. This hypothesis is, however, available when the vehicle speed is lower than the critical track/soil velocity. On the contrary, light transit vehicles, like trams or metros, are characterized by a low speed and a relatively high density of singular rail surface defects, like rail joints, rail crossings or even simple necessities like switching gears. The dynamic track deflection mainly contributes to ground wave generation. Between these two extremes, domestic intercity trains travelling at moderate speeds present excitation mechanisms that are a combination of those experienced on both high speed and urban railway lines. Quasi-static track deflection has a non-negligible influence on ground vibrations, in addition to its already present effects of singular defects.

As found in initial research in the area [2,18–20,29], HST’s present two notable characteristics: a high weight capacity (more than 10 tonnes per axle load) and a speed

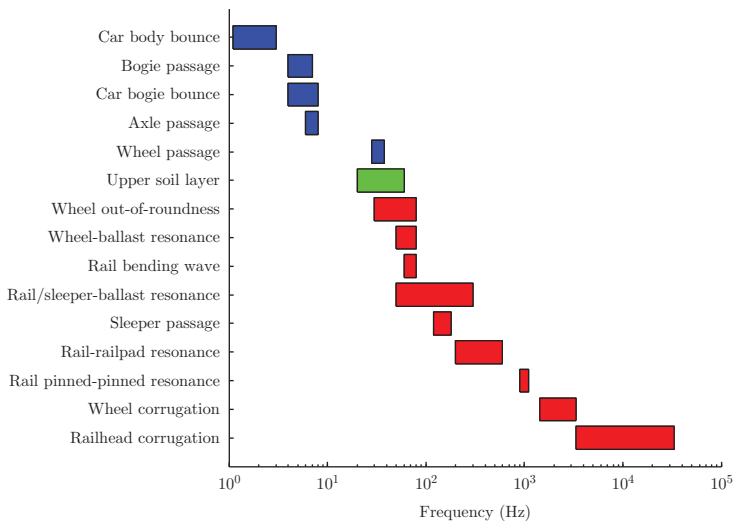


Figure 1. Main contribution of dynamic vehicle/track and soil interactions [80].

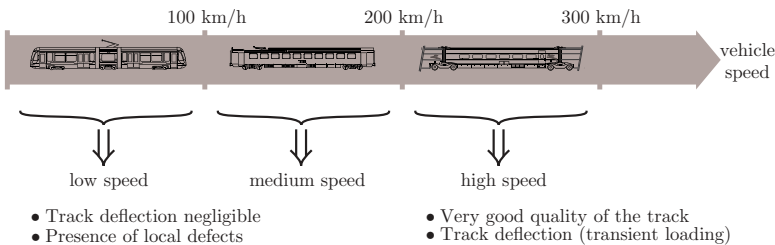


Figure 2. Synopsis of parameters influencing railway-induced ground vibrations.

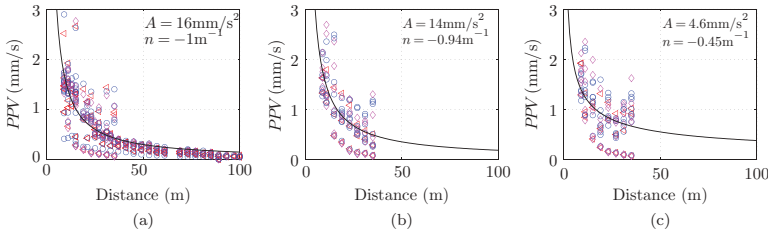


Figure 3. Peak particle velocity (*PPV*) collected on HSL sites in Belgium during the passing of HST (◦ : Thalys passing, ◁ : Eurostar passing, ◊ : TGV passing; solid line: best-fit curves of type Ay_R^n). (a) *z* direction, (b) *x* direction, (c) *y* direction.

that causes track deflection over a large frequency spectrum. Figure 3 presents typical values, expressed in terms of peak particle velocity (*PPV*), and obtained from recent experimental analyses in Belgium [81,82] for various HST types. The decrease in distance from the track is clearly emphasized, as is the case in other such studies [2,3]. Also, there is a large discrepancy between ground vibration levels (even for the same type of vehicle) even though the speeds recorded were between 281 and 304 km/h. It also becomes evident that vertical component vibration levels are similar to horizontal vibration levels, and in fact are dominant in some cases. This final observation is often neglected by most researchers who only study the vertical components.

Figure 4 shows the relationship between train speed, Rayleigh wave speed, and vibration levels. This data was collected for research on European high-speed lines, where the train speed was close to the soil Rayleigh wave speed. The horizontal axis shows a normalized train speed, which is equal to the train speed v_0 divided by the Rayleigh wave speed c_R , and is often called the Mach number. This number, defined as

$$M_R = \frac{v_0}{c_R} \tag{1}$$

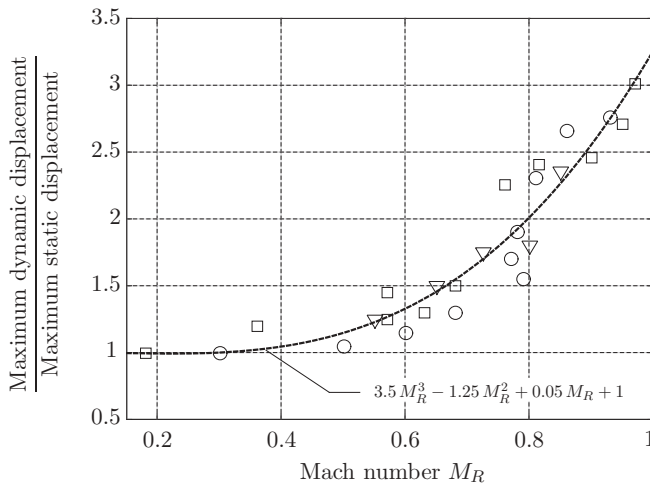


Figure 4. The effect of Rayleigh wave speed on vibration levels recorded on European sites (◦ : Ledsgard (Sweden); ▽ : Stilton Fen (UK); ◻ : Amsterdam–Utrecht (Holland) (issued from [86]).

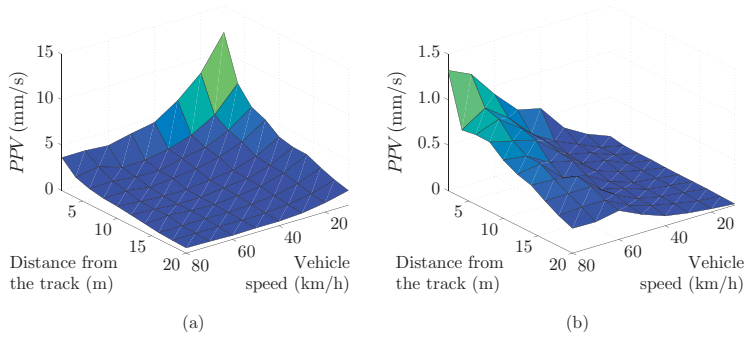


Figure 5. Vertical peak particle velocity (PPV) calculated from T2000 tram passing as a function of the distance from the track and of the tram speed [90]. (a) During the passing on the local defect, (b) during the passing on a rough rail (without local defect).

is here useful to classify the studied speed in sub- or super-Rayleigh cases. Therefore, a standardized train speed $M_R = 1$ is equivalent to a train travelling at the soil Rayleigh wave speed (critical velocity). The vertical axis is a measure of track vibrations portrayed by dynamic displacement, and then divided by static displacement. It can be noted that, when the normalized train speed exceeds 0.5, vibration levels (expressed as displacements) start to increase rapidly. This effect was also studied using numerical models to verify this statement in correspondence to elastic foundations [83], or to corroborate with ground vibration data [4,22,23,29,78,79,84,85]; most of these studies used the case of X-2000 HST running in Ledsgard (Bombardier, Västerås, Sweden).

The case of light rail vehicles has not been intensely studied, compared to the HST case. Despite this, it is important due to the close distance between the track and the buildings. The case of underground railways is also of a growing importance [38,46,67,87]. Typically, low-vibration mitigation solutions are analysed [24,88] with simple prediction models by characterizing their efficiency in a large frequency range. However, there is rarely a complete simulation procedure that combines the vehicle, track, and soil carried out. Kouroussis et al. [10,89,90] first focused their study on the T2000 tram circulating in Brussels, which received a large number of complaints. The analysis of characteristic vehicle effects on ground vibrations, or the quality of rail surface (Figure 5), can be retained as major findings from their work.

4. Track and soil dynamics modelling – considerations and assumptions

The simulation of unbounded domains in numerical methods is a very important topic in dynamic soil-structure interaction and wave propagation problems. This section provides a basic analysis of track and soil dynamic behaviour, and but is yet detailed to understand the essential mechanisms of ground vibration generation.

4.1. Linear analysis

Train traffic induced vibrations are mainly caused by the axle loads of vehicles passing on top of tracks with an uneven surface. A static and dynamic component can be defined for the axle load. The static component is due to the weight of the vehicle, and the dynamic component depends on the interaction between the vehicle, the track, and the soil.

Dynamic soil-structure problems involve waves propagating in the soil, but its dynamic response is more complex than that. Soil is composed of solid particles, water, and air. Its mechanical behaviour is essentially dependent on the correlation between the size of its solid particles and its cavities. Nevertheless, the non-linear behaviour of the soil is often neglected when the shear strain is inferior to 10^{-5} , as in cases of vibrations induced by railway traffic. In various applications, the soil can be modelled as a homogeneous or layered half-space, and is most often modelled as an elastodynamic medium.

4.2. Wave propagation

The pioneering work of Lamb investigates the response of isotropic and homogeneous elastic half-spaces compared to various harmonic and impulsive loads. By way of review, the principal features of the responses of an elastic half-space to point loads is discussed briefly [91,92].

If an oscillating point load is applied to an unloaded elastic half-space, three types of waves will emanate from the loading point. Surface waves, called ‘*R*-waves’ (or Rayleigh waves), decrease in the far field at a rate inversely proportional to the square root of the surface’s distance. The other two waves are related to body waves. The compression waves, called ‘*P*-waves’, and the shear waves, called ‘*S*-waves’.

The faster waves are the *P*-waves, while the *S*-waves are a somewhat faster than the *R*-waves (the speeds are in the order $c_P > c_S > c_R$). When analysing the interior of the elastic space, both body wave types decrease in amplitude in a manner inversely proportional to the spherical distance from the source point. When monitored on the surface, the body waves’ amplitudes decrease in a manner inversely proportional to the square of the surface distance. At the surface, *R*-waves are the predominant waves. For the partition of energy into the three types of waves, the order of magnitude is typically 67% for *R*-waves, 26% for *S*-waves, and 7% for *P*-waves [93].

This representation is, however, theoretical. The ground is, by nature, comprised of several layers, each one with specific properties. If the elastic and linear behaviour is retained for each layer, then it becomes possible to extend this wave approach to each layer; defined either by its Young’s modulus E_i (or shear modulus G_i), its Poisson’s ratio ν_i , and its density ρ_i (i being the index of the studied layer). For each layer, the *P*-wave velocity $c_{P,i}$ and *S*-wave velocity $c_{S,i}$ are deduced from

$$c_{P,i} = \sqrt{\frac{2G_i(1 - \nu_i)}{\rho(1 - 2\nu_i)}} \quad (2)$$

and

$$c_{S,i} = \sqrt{\frac{G_i}{\rho_i}} \quad (3)$$

A surface wave exists, but, in contrast to homogeneous soil, its velocity depends on frequency (the term ‘Rayleigh waves’ is often misused in this case, but generally refers to surface waves). Soil damping is also an important parameter influencing the soil response. Its modelling representation depends on the simulation approach. Frequency analysis

offers work with hysteretic and viscous models, while time domain simulation is restricted to viscous behaviour.

A layered soil response of stationary and moving loads can be analysed using seismographs [94], transfer functions [79], or dispersion diagram [20,95,96]. The latter presents a useful tool to analyse the propagating modes of the ground as a function of frequency, even on a series of recorded velocity traces due to a transient force. Figure 6 illustrates this statement by presenting dispersion diagrams for two examples of soil configuration (one homogeneous soil and one layered soil) when an impulse load is applied. The response for each frequency is normalized to the maximum value at that frequency, as proposed by Triepaischajonsak et al. [96], and allowing for a clear recognition of the corresponding wave numbers. The maximum value indicates the modal wave numbers that are vertically extended and follow straight lines (from the origin to the point on its dispersion curve at that frequency) corresponding to the inversion of wave speed. The effect of soil layering is also depicted in the following section, and Figure 6(b) displays the results for layered soil configuration. It can be observed that high-frequency content follows the characteristics of the upper layer, while low frequencies are associated with the substratum. The passage between the two reference lines corresponds to the oscillating frequency of soil surface, characterized by [95]

$$f_{\text{layer}} = \frac{c_{P,1}}{4d} \quad (4)$$

where $c_{P,1}$ is the compression wave velocity of the first layer of depth d . This frequency is equal to 20Hz for the example proposed in Figure 6(b).

4.3. Track modelling

Modelling train passage requires simulating seismic wave propagation through a track structure, and then into the ground. Rather than attempting to simulate vibration levels at distances from the track, early railway approaches focused primarily on vibration

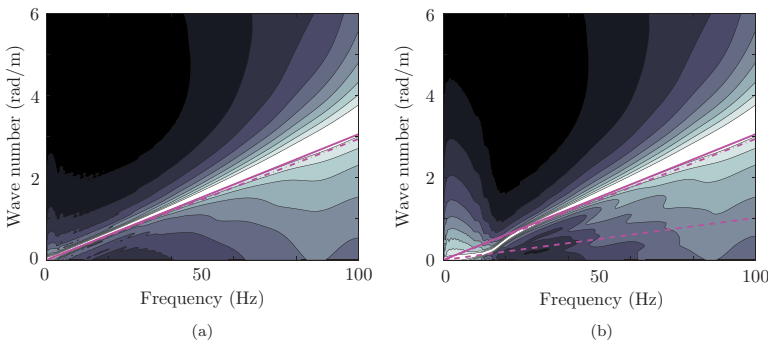


Figure 6. Dispersion diagrams obtained with FEM simulation (light: high amplitude; solid line: Rayleigh wave speed of upper layer; dash-dot line: shear wave speed of upper layer; dashed line: shear wave speed of the substratum). (a) Homogeneous soil configuration – $c_P = 398$ m/s; $c_S = 213$ m/s. (b) Layered soil configuration – $c_{P_1} = 398$ m/s; $c_{S_1} = 213$ m/s; $c_{P_2} = 1500$ m/s; $c_{S_2} = 612$ m/s; $d = 5$ m.

levels within the track's structure. This was a fundamental issue to railway track operators and designers. When attempting to model track vibration, the complex wave fields generated by the three-dimensional track geometries (e.g. sleepers) are difficult to model, particularly when using analytical expressions. To overcome these challenges, early analytical approaches simplified the track structure by making assumptions regarding track geometry; assuming at first approximation that a bi-dimensional model in a vertical plan along the track is sufficient to model the vehicle/track interaction. It was also assumed that vertical loading dominates the railway-induced ground vibration response.

Two categories of track are most commonly used for dynamic behaviour, (1) where the rail is assumed to be continuously supported or (2) where the rail is assumed to be discretely supported. This distinction is established by the discrete nature of sleepers along the track's direction. In both cases, the rail is treated as a flexible beam, which can be interpreted as infinite (the problem is solved in the frequency/wave number domain) or finite (more suitable for time domain simulation).

One of the most straightforward approaches to rail modelling is to use a Euler beam. Although Grassie et al. [97] concluded that this model is deficient in several respects in the frequency range 50–1500Hz, the difference shown when advanced modelling is used (Timoshenko beam, including shear deflection and rotational inertia of the rail) is negligible for frequencies below 500Hz. Continuously supported models are intended to simulate the entire track and neglect the effect of sleepers. To overcome this problem, sleeper effects can be modelled with the use of a intermittent support, facilitating superior accuracy at higher frequencies. A discrete support has multiple layers representing rail pads, sleepers, ballast, subballast, and subgrade. Such models can be solved in both frequency and time domains, however, frequency domain solutions are limited to linear behaviours inside the track's structure.

Figure 7 plots a typical vertical track displacement, showing three track modes that have been observed through experience:

- an initial resonance frequency considering where the rail and the sleepers vibrate in phase (called the $T1$ mode – under 100Hz in the figure),
- a second mode ($T2$ mode) where rail and sleepers vibrate out of phase (at 350Hz), and
- the third mode, called the pinned-pinned resonance ($P-P$ mode), where the rail vibrates with a wavelength equal to two sleeper bays (close to 800 Hz).

Knothe and Grassie [98] presented existing track models as functions of discrete or continuous nature of track support. The number of layers is also used to distinguish the masses of each component (sleeper, rail, ballast). This way of classifying components has not met any drastic changes since it was first proposed, and is still a measure that remains used today.

Track elements also play an important role in track dynamics. The railpads' role is to absorb a segment of rail vibrations, and to allow the movement of rails without damaging the sleeper. Various railpads have been studied, typically on the basis of their stiffness, and to a lesser extent on their damping [78]. The $T1$ and $T2$ mode's location changes with railpad stiffness, but the main effect is on the $T2$ mode.

The sleeper is another essential element of the track. It has two main roles: to transfer loads from the rails to the track ballast and the ground underneath, and to maintain the rail gauge. Spacing is limited and is usually restricted to 0.60m but, for the low-loaded

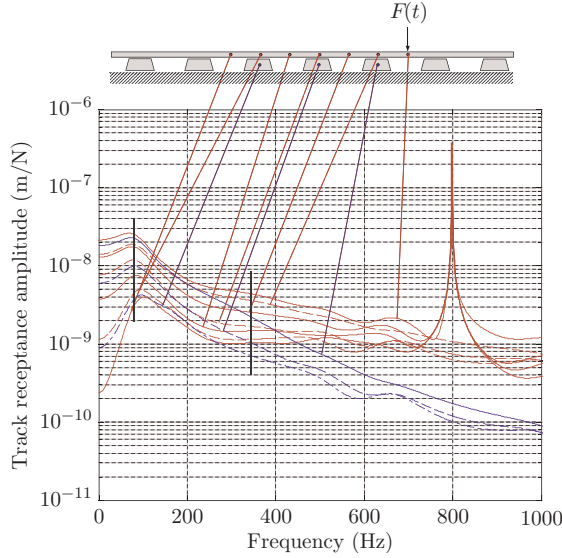


Figure 7. Track receptances calculated under FEM code.

tracks, or tracks consisting of continuous welded rail, it goes up to 0.72 m. The spacing of the sleepers and their mass only affect the $T1$ and $T2$ track modes. The spacing also changes the track $P-P$ mode. Ballast is used to facilitate drainage of water, and to distribute the load from the railroad ties, without distorting the settlement. As for the railpad, a simple spring element is sufficient to capture its main dynamic behaviour. Eigenfrequencies of $T1$ and $T2$ modes change as a function of stiffness but, in comparison to the railpad, both modes are affected in the same manner and in the same proportion [78]. Other authors, such as Zhai [99] or Ahlbeck [100], suggested working with an additional mass defining the inertia property of the ballast, in order to work with a 3-layer track model. Each mass defines a fictitious volume of ballast, behind each sleeper, and can be calculated as

$$m_b = l_s h_b \rho_b (l_e + h_b \tan \alpha) \quad (5)$$

where ρ_b is the apparent density of the ballast, the other terms are geometrical data (Figure 8(a)). The ballast stiffness is given by [99]

$$k_b = \frac{2E_b \tan \alpha (l_e - l_s)}{\ln \left(\frac{l_e (l_s + 2h_b \tan \alpha)}{l_s (l_e + 2h_b \tan \alpha)} \right)} \quad (6)$$

where E_b is the ballast Young's modulus. In order to include the coupling between 'ballast blocs', Zhai [99] suggested developing a discrete, classical model with additional spring and damper elements (k_w , d_w), all working in shear motion (Figure 8(b)). This idea is novel, but induces an additional difficulty in quantifying these values (five in total without taking into account the bloc geometrical values). The same model also presents the foundation flexibility through spring/damper elements (k_f , d_f). Other ballast modelling

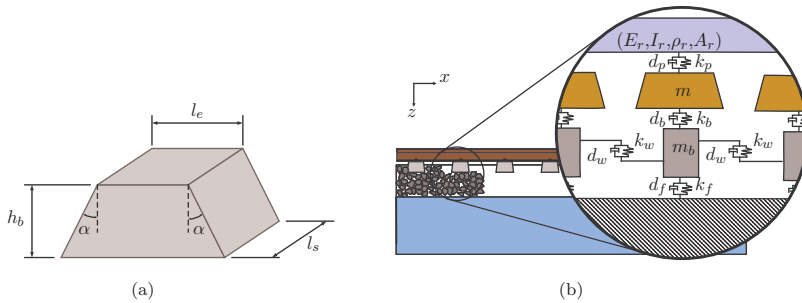


Figure 8. Zhai's model for dynamic behaviour of ballasted track according to [99]. (a) Geometrical ballast model, (b) 3-layer model for the track.

approaches exist, including volume continuity models where the ballast is considered an elastic linear, and discrete element modelling approaches using granular theory [101].

Early track models used Winkler [102] or viscoelastic [103] foundations, however, more recent elastic, half-space models have been shown to offer greater accuracy [104]. These latter models present more accurate results due to the improved coupling between the track and the foundation, and explain why almost all prediction models combine track and soil submodels in a single system. However, it is possible to make a reasonable and accurate assessment of the track/foundation pairing using lumped mass models together with viscoelastic elements, especially when it comes to the dynamic interaction between the track and the soil [105].

4.4. Three types of predictions soil models

Figure 9 presents the soil model classification proposed in this paper, based on analytical and numerical techniques to resolve dynamic soil problems.

Although analytical expressions exist to describe wave propagation, they typically require many assumptions to be used and for the excitation to remain stationary. Therefore, although they can be useful for validating more advanced numerical methods, they are usually not used for solving railway wave propagation problems.

The finite difference time domain (FDTD) method [106,107] is a numerical method that uses a strong formulation of the seismic wave equations to simulate wave propagation. It has gained wide acceptance in seismic exploration where it is the underlying tool used to perform full waveform inversions. It has also been used to predict railway vibrations [65,108]. Its strengths are that computations can be performed relatively quickly and although absorbing boundaries are required to prevent boundary reflections, high-performance PMLs (perfectly matched layers) are easily implemented. The disadvantage of using FDTD method for railway problems is that complex geometries, particularly near free surfaces are difficult to model. Therefore, modelling the track and an accurate excitation are challenging.

The finite element method (FEM) [109–111] is an alternative method that has gained wide acceptance in structural and vibration modelling. It has been used widely for railway vibration problems due to its versatility. It uses a weak form of the seismic wave equation and can easily model complex geometries. Furthermore, it is well suited to explicitly modelling structures/buildings close to the line. Despite this, it is not as computationally efficient as FDTD method and as the domain size is increased the run times become

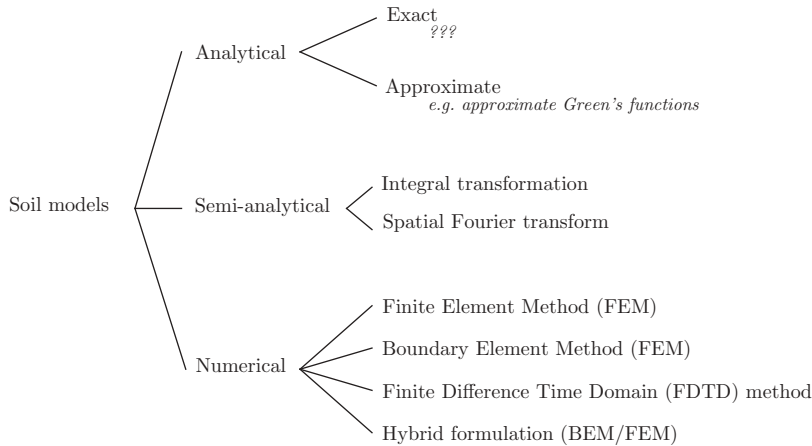


Figure 9. Soil models classifications.

prohibitive. Therefore, modelling large offsets can be challenging. To reduce the computational workload, the FEM can be reformulated in the frequency domain rather than the time domain. The challenge with this approach is that absorbing boundary conditions are difficult to implement in the frequency domain.

In an attempt to model wave propagation at large offsets, the FEM has been coupled with the BEM [112–114]. BEM uses Green’s functions to efficiently calculate vibration propagation at large offsets. Therefore the FEM is typically used to model the complex track arrangement and near-field vibration whereas the BEM is used to simulate the far-field vibration. A drawback of the BEM is that although soil vibration can be calculated in the boundary element regions, it can become challenging to calculate structural vibration in the same region. Also, when the large matrix formulation associated with the BEM is coupled with the FEM, the resulting computational power required may become prohibitive.

Alternatives to using the FEM/BEM include the scaled boundary finite element method (SBFEM) [115,116] or finite element thin layer method (FETLM) [117]. These approaches use a series of horizontal thin layers to prevent boundary reflections in the frequency domain. This allows the finite element equations to be formulated in the time domain to reduce computational effort, while facilitating efficient boundary absorption. Therefore these approaches are currently attracting significant attention.

5. Vehicle modelling using a sequence of constant axle loads

Although a sequence of travelling axle loads is a simplistic way to define a vehicle and its effect on a track, it provides information about the generation of ground vibrations. We can clearly distinguish track deflection (and the associated spectrum), as well as physical interpretation of effects related to critical velocities (vehicle speed close to critical track/soil velocity).

5.1. Track deflection

To analyse track deflection due to the moving weight of a vehicle in simplified terms, a plain track/foundation model is sufficient. Grassie et al. [97] demonstrated that a track

resting on a simple elastic support is satisfactory for low-frequency excitation (up to 100Hz in the studied case). This statement has been confirmed in [8] by comparing this theoretical approach to a track finite element model. In a series of papers [17,18], Krylov proposed an analytical method which makes it possible to determine the deflection $w(x, t)$ of the track subjected to a load P moving at a constant speed v_0 . The following Euler formulation is used to represent the behaviour of the track

$$E_r I_r \frac{\partial^4 w}{\partial x^4} + K_f w = P \delta(x - v_0 t) \tag{7}$$

The track (two parallel rails with periodically fastened sleepers) is treated as an Euler–Bernoulli elastic beam (Young modulus E_r , cross-sectional momentum I_r) lying on a Winkler foundation, defined by its stiffness K_f per unit of length, including railpad, ballast and, foundation contributions. The solution of Equation (7) is written as

$$w(x, t) = w(x - v_0 t) = \frac{P}{8E_r I_r \beta^3} e^{-\beta|x - v_0 t|} [\cos(\beta|x - v_0 t|) + \sin(\beta|x - v_0 t|)] \tag{8}$$

where $\beta = \sqrt[4]{\frac{K_f}{4E_r I_r}}$ is introduced, representing a ratio of flexibility between the foundation and the rail.

Theoretical rail deflections, often called quasi-static deflections, are presented in Figures 10–13, and take into account the number of carriages for each studied vehicle. The geometrical configuration of these studied vehicles is given in Appendix. Periodicities of wheel sets, bogies, and carriages are defined as

$$f_a = \frac{v_0}{L_a} \tag{9}$$

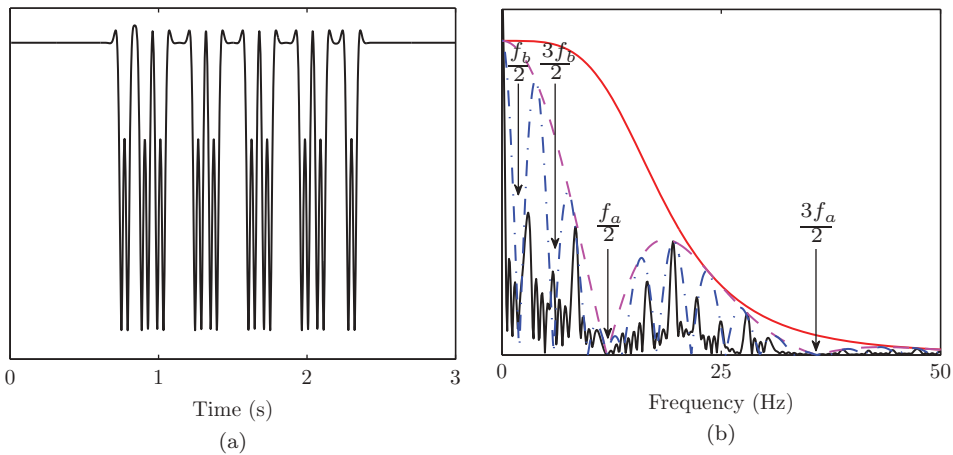


Figure 10. Track deflection due to the moving of a X2000 HST vehicle ($L_c = 24.96\text{m}$, $L_b = 17.70\text{m}$, and $L_a = 2.90\text{m}$) at speed $v_0 = 250\text{km/h}$ (solid line: single wheel set; dash line: single bogie; dash-dot line: entire carbody). (a) Time history, (b) frequency content.

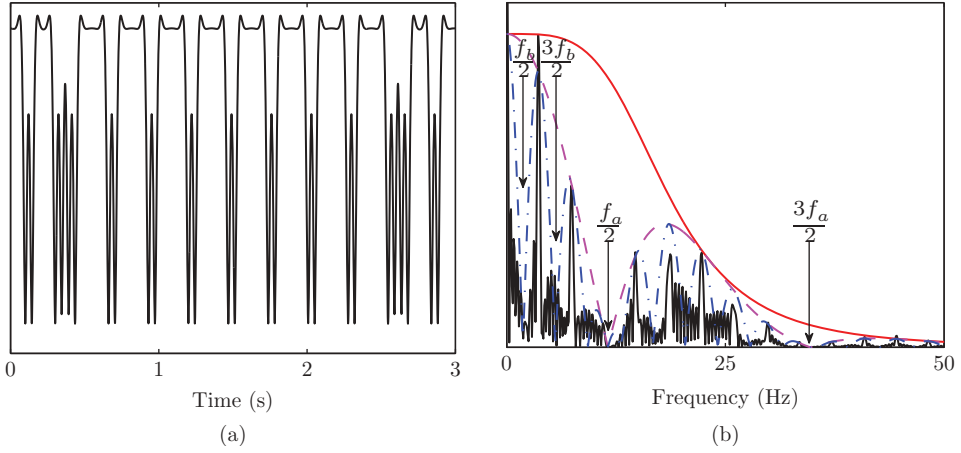


Figure 11. Track deflection due to the moving of a Thalys HST vehicle ($L_b = 18.70\text{m}$ and $L_a = 3.00\text{m}$) at speed $v_0 = 250\text{km/h}$ (solid line: single wheel set; dash line: single bogie; dash-dot line: entire carbody). (a) Time history, (b) frequency content.

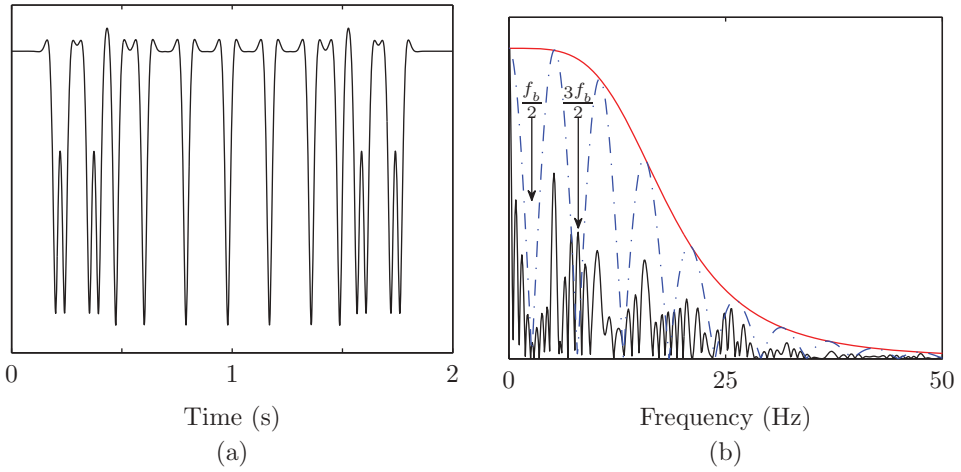


Figure 12. Track deflection due to the moving of a Talgo 250 HST vehicle ($L_b = 13.14\text{m}$) at speed $v_0 = 250\text{km/h}$ (solid line: single wheel set; dash-dot line: entire carbody). (a) Time history, (b) frequency content.

$$f_b = \frac{v_0}{L_b} \quad (10)$$

$$f_c = \frac{v_0}{L_c} \quad (11)$$

depending on the wheel set spacing L_a , bogie spacing L_b , and carriage length L_c , and are presented on these graphs. The case of the X2000 HST (Figure 10) illustrates these periodicities.

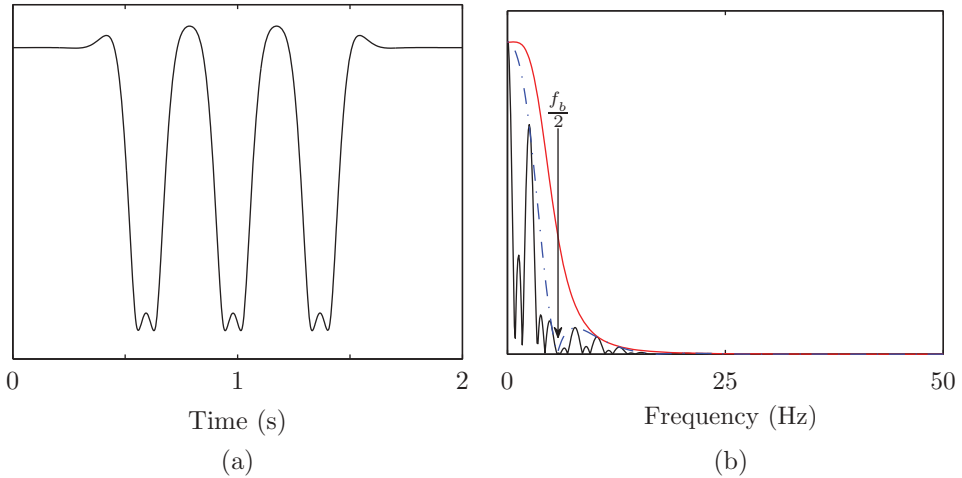


Figure 13. Track deflection due to the moving of a T2000 tram ($L_b = 7.52$ m and $L_a = 1.70$ m) at speed $v_0 = 70$ km/h (solid line: single wheel set; dash-dot line: single bogie). (a) Time history, (b) frequency content.

A first inflection is apparent due to the fundamental axle passage frequency f_a at regular frequency intervals with zero amplitude at frequencies $\frac{2k+1}{2}f_a$ ($k \in \mathbb{N}$). A second amplitude inflection is due to the fundamental bogie passage frequency f_b , with zero amplitude at $\frac{2r+1}{2}f_b$ ($r \in \mathbb{N}$). The dominant frequencies defined by Equation (11) have maximum amplitudes following the last envelope. The frequency range, defined by the first envelope, demonstrates how vibration magnitude decreases proportionally with frequency. The cut-off frequency depends on β and more particularly on foundation flexibility K_f , since the rail flexural stiffness $E_r I_r$ does not vary on a large scale. Increasing the speed v_0 results in the cut-off frequency becoming more dominant (the rail deflection contributes to an impulse Dirac delta). Similar conclusions can be drawn for other vehicles; namely the Thalys HST (Figure 11), Talgo 250 HST (Figure 12), and the T2000 tram (Figure 13) with notable points:

- A greater (smaller) number of carriages induces more (less) pronounced dominant frequency peaks.
- If $L_c = L_b$ (Jacob's bogie particularity on Thalys HST), the dominant frequencies follow the modulated maximum amplitude.
- The effect of locomotives, which present a different geometrical configurations, have a non-negligible role on the amplitude modulation, which is more complex.

These observations are in accordance with [5,118,119]. Dominant frequencies are of relevant interest when it comes to ground vibration studies, and also offer additional applications, such as methods of train speed calculation [80,120].

5.2. Introduction of critical speed

Critical railway speeds can also be studied using a simple track model, by introducing the tracks' mass. Equation (7) is updated by taking into account the track inertia:

$$E_r I_r \frac{\partial^4 w}{\partial x^4} + m_r \frac{\partial^2 w}{\partial t^2} + K_f w = P \delta(x - vt) \quad (12)$$

The track is modelled as a beam with a uniform mass m_r per unit length, at the same time representing the rail and sleeper masses [17,121] on a Winkler foundation. The vertical deflection is therefore equal to

$$w(x - v_0 t) = \frac{P}{8E_r I_r \beta^3 \xi} e^{(-\beta \xi |x - v_0 t|)} \left[\cos(\beta \psi |x - v_0 t|) + \frac{\xi}{\psi} \sin(\beta \psi |x - v_0 t|) \right] \quad (13)$$

by introducing the minimal phase velocity of bending waves multiplying in a system track/ground

$$v_{\min} = \sqrt[4]{4k_f E_r I_r / m_r^2} \quad (14)$$

which is required for the non-dimensional parameters

$$\xi = \sqrt{1 - (v_0 / v_{\min})^2} \quad (15)$$

$$\psi = \sqrt{1 + (v_0 / v_{\min})^2} \quad (16)$$

The dynamic effect of the track can be analysed, with a vehicle/track resonance developing if the train speed approaches this minimum phase velocity.

This analytical approach is an interesting way to introduce critical speed, but neglects soil critical velocity as a contribution to the dynamic effect. From the viewpoint of the soil, other speeds have been defined as critical. By considering an unbounded elastic body (i.e. no free surface, thus no surface wave propagation), there are three distinct velocity regimes:

- (1) The subsonic case – the load moves at a speed less than the shear wave speed of the material constituting the half-space ($v_0 < c_S$).
- (2) The transonic case – the load moves at a speed greater than the shear wave speed but less than the compressional wave speed ($c_S < v_0 < c_P$).
- (3) The supersonic case – the load moves at a speed greater than the compressional wave speed ($v_0 > c_P$).

The reformulated, unbounded elastic body solution for a moving line load on an elastic half-space provides additional information. The presence of a free surface causes the generation of Rayleigh surface waves, after which it is possible to show that when the load reached a speed equal to the R -wave speed c_R , the displacement becomes indefinitely large. As R -waves are dominant during train passage, this result is of specific concern to the railway industry. The aforementioned classification can be extended to the Rayleigh wave velocity, where two additional regimes can be added before reaching the subsonic case:

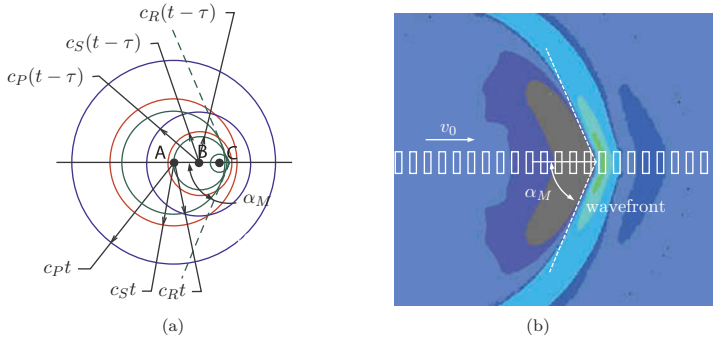


Figure 14. Subsonic and super-Rayleigh state for a moving load (bird's-eye view). (a) Theoretical wave front, (b) Soil surface motion obtained with FEM.

- For a load speed less than the Rayleigh wave velocity, the regime is considered as sub-Rayleigh.
- For a load speed greater than the Rayleigh wave velocity, the regime is called super-Rayleigh.

These terminologies were developed from aeroacoustic phenomena. Similar to the aeroacoustic industry, the first researchers working on the critical speed of solid media introduced non-dimensional speeds, using the concept of the Mach number (as already shown in Equation (1)):

$$M_i = \frac{v_0}{c_i} \quad \text{with } i = P, S, \text{ or } R \quad (17)$$

A moving train load can be estimated as a series of point loads acting on a rail surface at different locations and different instances of time. Since the rail is discretely supported by sleepers, the forces acting on the sleeper can be seen as a sequence of forces acting with a delay, and regularly displaced at the surface level. Bending waves propagate in a track/ground system, as well as body and surface ground waves generated at all excitation points, which arrive at the receiver at a specific moment in time. In practice, the minimum phase velocity is greater than the Rayleigh wave velocity, so this allows for greater focus on the ground waves problem. Figure 14 illustrates this theory by comparing the response observed at a certain location with the function of all the seismic waves (Figure 14(a)) and an alternative numerical visualization (Figure 14(b)) obtained from a finite element analysis, which includes the vehicle/track and track/soil interaction [79]. It is clearly evident that the maximum vibration is concentrated in a cone, and determined by the wavefront angle, the so-called Mach angle, which can be calculated by

$$\alpha_M = \arcsin \frac{1}{M_R} \quad (18)$$

6. Vehicle modelling using a sequence of randomly varying axle loads

6.1. Dynamic axle loads

The previous section focused on quasi-static excitation, akin to static excitation, where the vehicle's speed is adequately lower than the critical track and soil speed. In practice, rail

and wheel surface imperfections play a role on wheel/rail forces, which are important for examining dynamic excitation in the evaluation of railway-generated ground vibrations.

A significant enhancement in the sequence of a constant axle load is to include a random dynamic response to the track static displacement, which is associated with the wheel/rail unevenness

$$w(t) = w_{st}(t) + w_{dyn}(t) \quad (19)$$

where $w_{st}(t)$ is the track deflection due to axle loads, and $w_{dyn}(t)$ the track displacement induced by the irregular track or/and wheel surface contact. Although an uncommonly used approach, it provides detailed insights if the axle load is based on the assumption of perfect contact between the train and the track. It was successfully used by Lu et al. [25] to present an efficient algorithm for problems of coupled vehicle/track systems which were subject to random moving loads. Lombaert et al. [27] applied this method to a numerical model for the prediction of railway-induced vibrations, in order to evaluate the contribution of dynamic excitation versus quasi-static excitation with a moderate computational cost. This approach was successfully developed for the calculation of domestic and HSTs in Belgium.

The key challenge with this methodology is to distinguish between the unevenness of the track and the wheel. The following sections present a summary of existing possibilities in assessing this information.

6.2. Rail unevenness

6.2.1. Spatial versus time domain modelling

When defects in the rail surface cannot be recorded by means of a track geometry car, the use of analytical representation is often accepted as it is typically based on collected data and experience. Track geometry is defined in terms of four types of irregularity [122]:

- the gauge, defined as the horizontal distance between two rails,
- the cross level of difference in elevation between two rails,
- the alignment of an average lateral position and
- the vertical profile for an average elevation of two rails.

In the case of ground vibrations, only the vertical profile is studied, since it plays an important role in vertical track dynamics, and is suitable for quantifying any unevenness of the rail. It is defined as a random function $z(x)$ from space x . Its distribution is often based on a statistical form, which uses power spectral density (PSD) $S_{zz}(\phi)$, as a function of the spatial frequency ϕ (number of cycles per unit of length, or of its inverse, the wavelength $\lambda = 1/\phi$). In vehicle/track dynamics, this kind of defect is considered a time history excitation, where the vehicle runs at speed v_0 . Each spatial function $z(x)$ corresponds to a time excitation $\tilde{z}(t) = z(v_0 t)$, for which it is possible to calculate a power spectral density $S_{zz}(f)$ in the frequency domain. Each affiliation comes from this statement (Table 2). More precisely, the correspondence between signal energy verifies the Parseval's identity

$$\int_{-\infty}^{+\infty} S_{zz}(\phi) d\phi = \int_{-\infty}^{+\infty} \tilde{S}_{zz}(f) df = \sigma^2(z) \quad (20)$$

Table 2. Relationships between spatial and time domains.

	Spatial domain		Time domain	
Abscissa	$x = v_0 t$	(m)	$t = \frac{x}{v_0}$	(s)
Frequency	$F = \frac{f}{v_0}$	(m ⁻¹)	$f = F v_0$	(Hz)
Circular frequency	$\Omega = 2\pi f$	(rad/m)	$\omega = 2\pi f = \Omega v_0$	(rad/s)
Rail surface defect	$z(x)$	(m)	$\tilde{z}(t)$	(m)
<i>PSD</i>	$S_{zz}(\phi)$	(m ³)	$\tilde{S}_{zz}(f)$	(m ² /Hz)

with σ^2 being the variance of z . Since $df = v_0 d\phi$, the link between these two densities is given by

$$\frac{S_{zz}(F)}{v_0} = \tilde{S}_{zz}(f) \tag{21}$$

6.2.2. Power spectral density

The distributed rail unevenness data has a well-defined shape, often described by [75]

$$S_{zz}(\Omega) = \frac{\mu}{\left(1 + \frac{\Omega}{\lambda}\right)^n} \tag{22}$$

The three parameters λ , μ , and n define the spectrum. However, only two parameters are used in practice: the amplitude parameter μ and the spread parameter λ ; n being typically comprised between 2 and 4. $n = 3$, has been adopted by Société Nationale de Chemin de fer Français (SNCF). The analytical spectrum defined by Equation (22) can be characterized by a shape function $\Phi(\Omega)$ such as

$$S_{zz}(\Omega) = \pi\sigma^2\Phi(\Omega) \tag{23}$$

with the statistical parameter σ^2 defined in Equation (20). This shape function is typically associated with track structure and nature of foundation. The change in variance also allows for evaluation of the unevenness of the rail when compared to the ageing of the track.

Amid the many proposed definitions of the unevenness rail spectra, a few examples were individually selected for this review:

- **Level Deutsche Bahn (DB) — SIMPACK** [123]: The multibody simulation software package SIMPACK AG (Gilching, Germany) offers the means for modelling random excitations in the wheel/rail or tyre/road contact through its library ‘time excitation generator’, with the help of shape filters represented by

$$S(\Omega) = \frac{b_0 + b_1 j\Omega}{a_0 + a_1 j\Omega + a_2 (j\Omega)^2} \tag{24}$$

It should be noted that $S(\Omega)$ is the root-mean square of *PSD* (demonstrating, among other things, the real difficulty in comparing these functions, in view of the

Hellenbroich [126], and later by Lombaert et al. [27] and Costa et al. [7] to provide an equivalent form for track irregularities, using the expression

$$S_{zz}(\phi) = S_{zz}(\phi_0) \left(\frac{\phi}{\phi_0} \right)^{-w} \tag{27}$$

where parameters $S_{zz}(\phi_0)$ and w are tabulated according to track qualities (ϕ_0 being a reference spatial frequency equal to 0.1 m^{-1}).

For simulations performed in a time domain, the PSD must be converted to an actual profile expressed in terms of position x . If $\Delta\phi$ is the resolution retained for the spatial frequency, the profile can be written according to the following Fourier series

$$h(x) = \sum_k \sqrt{2\Delta\phi S_{zz}(k\Delta\phi)} \cos(k\Delta\phi x + \phi_k) \tag{28}$$

where ϕ_k is randomly determined according to a uniform distribution between $-\pi$ and π .

Figure 15 presents these functions, and is used to quantify the difference in amplitude between these formulations. Although Garg and Dukkipati’s function is outdated, it is assumed that rail irregularity has not changed much through the years. It is advantageous in its ability to be more refined than Andersson’s or DB characterization.

Figure 16 shows vertical profiles generated in this way, using the PSD proposed by AAR. The link between these profiles and the domain of frequency depends, of course, on

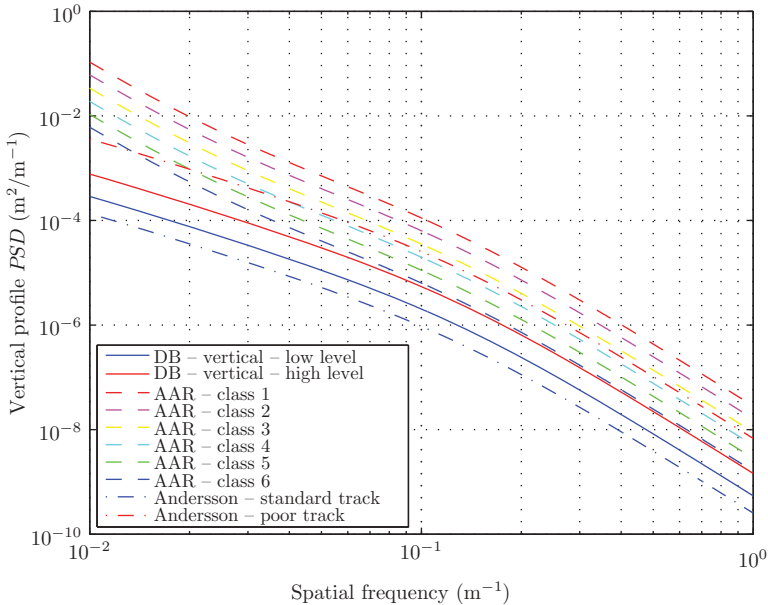


Figure 15. Analytical PSD functions representing the distributed rail unevenness.

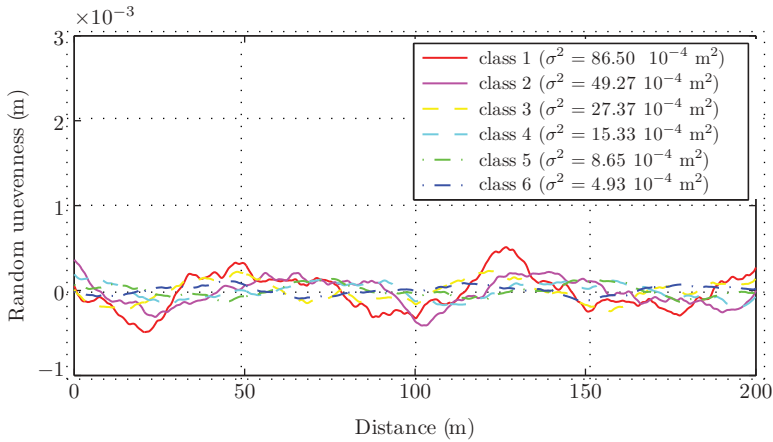


Figure 16. Generated unevennesses, based on the model of AAR.

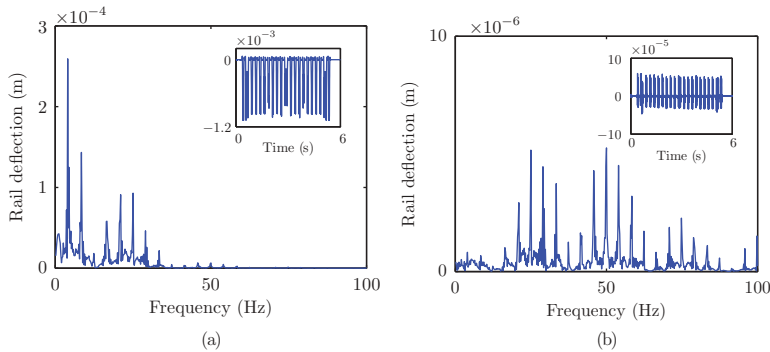


Figure 17. Example of static and dynamic track deflections calculated in the case of a Eurostar running at 300km/h (results from [8]). (a) Static track deflection w_{st} , (b) dynamic track deflection w_{dyn} .

the vehicle's speed, even though the latter is not affected by profile variation in the same way if it runs at 30 or 300km/h.

To illustrate the importance of rail unevenness on ground vibrations, Figure 17 shows the static and dynamic contributions in the rail deflection numerically obtained in the case of a Eurostar HST and illustrates the dynamic effect defined by Equation (19).

6.2.3. Singular rail surface defects

In practice, other spectra are added to the distributed rail unevenness spectrum, also called the 'background spectrum', and are connected to track design. Commonly, rail joints are necessary to prevent lateral or vertical movement of the rail ends, and allow for a range in movement of the rails for purposes of expanding or contracting. Other local rail surface defects exist, like turnouts or rail crossings, which have the same effect, and manifest themselves as a local geometries at the rail surface, which are

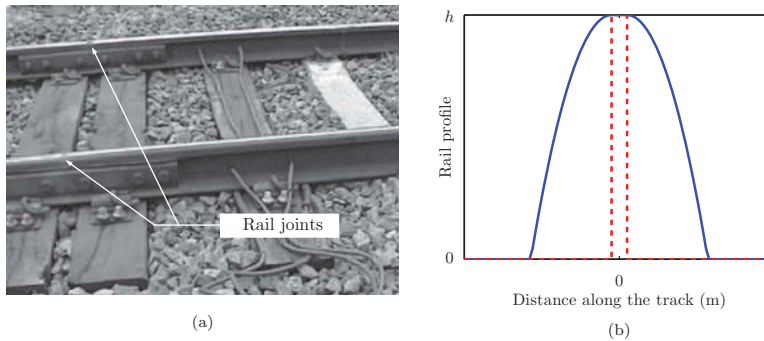


Figure 18. Characterization of a rail defect. (a) Example of rail joint on both rails at the same position along the rail. (b) Analytical representation (dash-dot line: defect shape; solid line: wheel contact point position).

influential in modifying the wheel/rail forces. These irregularities are most often encountered in traditional tracks, and more typically in urban environments (Figure 18(a)). Taking into account the wheel curvature (Figure 18(b)), analytical functions can be deduced in order to accurately present the legitimate raising of a wheel's contact point [127]. For more modern use, particularly where higher speeds are required, the lengths of the rail may be welded together to form continuous welded rails (CWR).

At this stage, an accurate description of the effect of a singular rail surface defect on a track and on the ground must be explained in greater detail, taking into account the representation of the vehicle/track interaction.

6.3. Additional wheel/rail contact irregularities

In addition to rail unevenness, several other types of irregularities can be taken into account. An example of such unevenness is the roughness of the wheel surface, the roughness of the rail surface, and the out-of-roundness of the wheel. Specific frequency ranges are associated with these defects [128]:

- from >10Hz for wheel out-of-roundness and roughness,
- from >50Hz rail roughness.

Regarding out-of-roundness, different types exist [129], including polygonal wheels, eccentricity, corrugation on block-braked wheel treads, and missing pieces of tread material owing contact to fatigue cracking. Corrugation is a result of the grinding of the wheel/rail interface, and produces wavelengths which may vary from 25 to 1500mm [130]. Wear is the only assumed active damage mechanism, and is caused by a longitudinal slip in the contact of the wheel and the rail.

Unfortunately, few ground vibrations problems have been analysed in literature, with most researchers trying to develop devices for measuring these defects, and to analyse the acoustic nuisances generated, or find a solution to minimize their development [131–134]. However, typical amplitude spectra in one-third octave bands are provided by these authors.

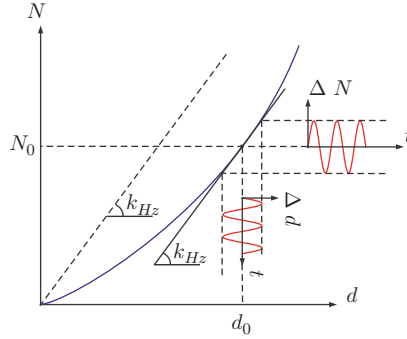


Figure 19. Wheel/rail contact: Hertz's theory and linearization.

7. Detailed models of the vehicle modelling

7.1. Wheel/rail contact

One of the main concerns in railway dynamics is the modelling of wheel/rail contact. With the advancements of Kalker [135], railway simulation in this area has developed quickly. For vertical loading, wheel/rail contact is defined by non-linear Hertz's contact stress law, comprising of the non-linear relationship between the imposed load N and the material deformation d

$$N = K_{Hz} d^{3/2} \quad (29)$$

where the coefficient K_{Hz} depends on the radii of arch between the wheel and the rail, and the elasticity of material for both bodies. A linearized model is often necessary for frequency domain analyses, by considering small variations Δd around the nominal value d_0 (Figure 19). Equation (29) can be approximated by the linear law

$$N = N_0 + k_{Hz} \Delta d \quad (30)$$

with $k_{Hz} = 1 \text{ GN/m}$ in most cases studied. k_{Hz} is obtained from the nominal force N_0 and the coefficient K_{Hz}

$$k_{Hz} = \left. \frac{\partial N}{\partial d} \right|_{d_0, N_0} = \frac{3}{2} K_{Hz} d_0^{1/2} = \frac{3N_0}{2d_0} \quad (31)$$

Nevertheless, most ground vibration models propose a linear adaptation of this contact, at a current moment in time, neglecting the dynamic contact behaviour for large variations of a wheel/rail force. Equation (30) is often misused in some ground vibration models by omitting the nominal force N_0 , and instead applying a simple proportionality using the N - d law.

7.2. Lumped mass models

Since many vibration standards [136–138] consider that low-frequency vibrations as having the most critical effect on buildings and human exposure, it is important to

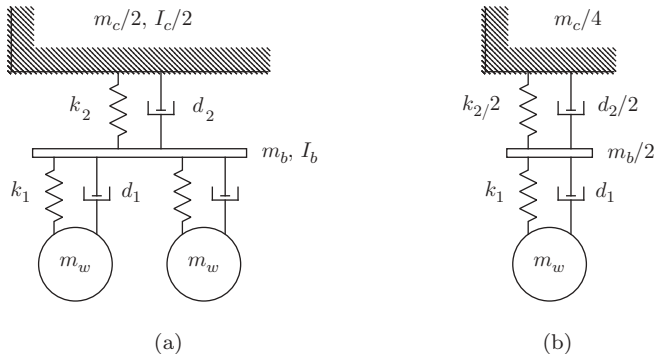


Figure 20. Simple dynamic models adopted for the vehicle (m_c : carbody mass; m_b : bogie mass; m_w : wheel set mass; I_c : carbody pitch inertia; I_b : bogie pitch inertia; k_1 : primary suspension stiffness; k_2 : secondary suspension stiffness; d_1 : primary suspension damping; d_2 : secondary suspension damping). (a) 1/2-vehicle, (b) 1/4-vehicle.

include ground vibrations affected by vehicle simulations as part of the problem. Taking into account vehicle unsprung, semi-sprung, and sprung masses interconnected by spring and damper elements from a finished vehicle, it is possible to develop a basic model, representing the primary and secondary suspensions. A 1/4-vehicle model is then derived from this model (Figure 20). The limitation of this approach is twofold: complex models are difficult to couple with track/soil models in order to predict ground vibrations, and values of vehicle dynamics parameters are difficult to obtain from the manufacturers. Based on Figure 20(b), a linear system of equations of motion is defined as

$$[\mathbf{M}_v] \{\ddot{\mathbf{q}}_v\} + [\mathbf{C}_v] \{\dot{\mathbf{q}}_v\} + [\mathbf{K}_v] \{\mathbf{q}_v\} = \{\mathbf{f}_v\} \quad (32)$$

where \mathbf{M}_v , \mathbf{C}_v , and \mathbf{K}_v are the mass, damping, and stiffness matrices, respectively. The external forces (essentially the gravity forces) are accounted for in vector \mathbf{f}_v . Configuration parameters \mathbf{q}_v are coupled to the track ones, through Hertzian contact defined by Equation (29) or Equation (30). Two types of lumped mass models can then be defined, based on the nature of Hertzian contact. A linear model is often used when the whole prediction model works in the frequency domain [29,63,64,139]. A non-linear one is more custom for time domain simulations [48,52–54,89].

Studying ground vibrations with a more detailed model of a vehicle is not futile because moderated abatement measures can be applied to the vehicle itself. To accomplish this, the dynamic behaviour of the vehicle together with the track and the soil must already be known. In [127], a modal analysis of the vehicle revealed that bounce and pitch mode eigenfrequencies strongly depend on the presence or absence of a flexible track. The same effect is also apparent for the ground. Mirza et al. [140] showed that an increase in vibration level was numerically observable for a stiffer primary suspension, and a heavier unsprung mass. Based on simulated results, Costa et al. [7] recommended the consideration of unsprung and semi-sprung (bogies) masses of a train in a prediction model, in order to significantly increase its accuracy. Specific studies also require a detailed model of vehicle and wheel/rail interaction, as is the case for the analysis of the flat wheel effect [141].

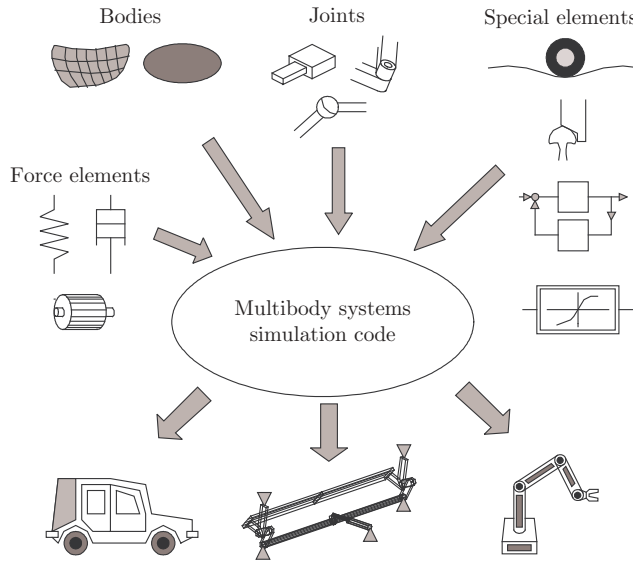


Figure 21. Principle of multibody simulation software.

7.3. Multibody approaches

To model vehicle behaviour constructors typically use generic multibody codes. A multibody system simulation code (Figure 21) allows the assembly of classical elements like bodies (either rigid or flexible), joints, and elements of force in order to build a model of the mechanical system being considered. Eventually, special elements are expected to encounter the characteristics of such applications. For example, wheel/rail contact elements in a railway case. The boundary between the multibody approach and the previous approach with lumped mass is not yet clear, but it could be somewhat rephrased to [142, p. 11]:

The elements of multibody systems for vehicle modelling include rigid bodies, which may also degenerate to particles, coupling with elements like springs, dampers or force controlled actuators as well as ideal, i.e. inflexible, kinematical connecting elements like joints, bearings, rails and motion controlled actuators. The coupling and connection elements, respectively, generate internal forces and torques between the bodies of the system, or external forces, with respect to the environment, and are generally defined as non-linear. Both of them are considered elements without mass. Each body motion may undergo large translational and rotational displacements.

Without limiting the analysis to linear behaviours (for example, wheel/rail contact), it appears that, although the rigid body definition prevents deformations of each mass, the multibody approach allows for the simulation of large displacements and rotations between individual bodies.

In order to analyse a multibody system, the spatial configuration of each body must be clearly defined. Once this position is known, velocities and accelerations can be obtained by derivation of forces (where inertia forces can be calculated) so that the equations of dynamic equilibrium can be developed. Generally, the first step when building a model of a multibody system is to choose a set of configuration parameters \underline{q} , in whose operation

each body will be determined. The nature of the configuration parameters typically depends on the type of coordinates used to express the kinematics of a system. Three main types of coordinates can be distinguished: minimal or generalized coordinates, relative coordinates, and Cartesian coordinates.

The approach based on *Cartesian coordinates* first considers independent bodies and then attributes each of them as many configuration parameters as needed (three or six parameters considered as planar or spatial) in order to acquire free motion in space. All joints are then systematically treated in a pattern of constraint equations. The configuration of a multibody system is, therefore, described by n Cartesian coordinates \underline{q}_v , and a set of l algebraic, kinematic, independent, holonomic constraints $\underline{\lambda}$

$$\begin{aligned} [\mathbf{M}_v(\underline{q}_v)] \cdot \{\ddot{\underline{q}}_v\} + [\mathbf{B}^T(\underline{q}_v)] \cdot \{\underline{\lambda}\} &= \{\mathbf{R}(\underline{q}_v, \dot{\underline{q}}_v, t)\} \\ [\mathbf{B}^T(\underline{q}_v)] \cdot \{\dot{\underline{q}}_v\} &= 0 \end{aligned} \quad (33)$$

where \mathbf{M}_v is the mass matrix associated with the Cartesian approach, \mathbf{B} is the Jacobian matrix of constraints, and \mathbf{R} is the vector of all the external forces acting on each body (excluding the joint forces).

If *relative coordinates* are used, the system will, in essence, be defined by a set of kinematic chains originating from the ground, or from a point of an existing chain. In each chain, the position of a body is placed with respect to the preceding one in the kinematic chain, with regards to coordinates expressing the relative position of both bodies. Similar equations of motion like Equation (33) are acquired.

The approach of *minimal coordinates* consists of choosing as many configuration parameters as the actual number of degrees of freedom in the system. The governing equations of the vehicle can be written in the following form

$$[\mathbf{M}_v(\underline{q}_v)] \cdot \{\ddot{\underline{q}}_v\} + \{\mathbf{h}(\underline{q}_v, \dot{\underline{q}}_v, t)\} = \{\mathbf{f}_v\} \quad (34)$$

where \mathbf{M}_v is the mass matrix, \mathbf{h} is a vector that aggregates the centrifugal and gyroscopic forces, due to the suspensions (springs and dampers), and wheel/rail contact. \mathbf{f}_v is a vector that describes the external forces (gravity), and \underline{q}_v describes the configuration parameters. If these equations are linear (or are linearized around their nominal position), a similar equation system to the one of Equation (32) is achieved.

A question soon develops when all of the previous research is taken into account: why work with 100 coordinates when the problem can be solved with only 10? The answer is simple: the smaller the size of the system the faster it will be to solve, but it will also take longer to build. In the case of a railway vehicle, the approach of minimal coordinates leads to a minimal number of equations, but setting up the latter approach is a long procedure as it requires a dedicated resolution of kinematics. With Cartesian coordinates, the number of equations is high but they can be easily composed. As a consequence, the best/worst depends not only on the system considered, but also on the integration scheme. Figure 22 presents an example of a vehicle model, taking into account the pitch motions of car bodies and bogies, and the bounce of the wheel sets (2D approach). For the proposed model, the already established approach of coordinates allows for the formation of equations of motion through a system of 10 equations. The Cartesian approach provides 21 differential equations, plus 11 algebraic equations, with an added problem of encompassing them with a specific integration scheme.

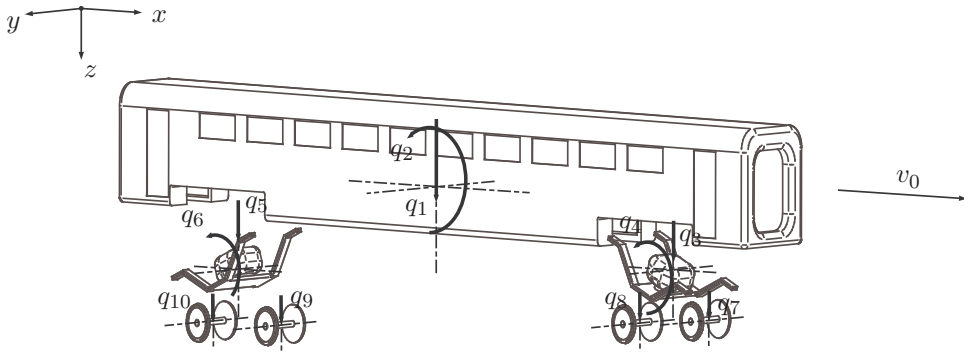


Figure 22. Vehicle modelling: configuration parameters highlighting.

Current dedicated modelling software packages in railway industry (Simpack, Vampire, ADAMS/rail, etc.) have collectively chosen the Cartesian approach, preferring the user-friendliness of the approach in dynamic simulation. Most of these tools are consequence of research and development activities. They have been verified through the use of different benchmarks (e.g. the Manchester Benchmarks [143]). At present, different computational procedures and methods developed by depicting vehicle interaction with neighbouring ones led to the development of several computer programs used by designers and analysts. For example, to study the effect of a vehicle running on bridges, Dietz et al. [144] used co-simulation of the vehicle/track system, considering a fixed model element for the track. Zhai and True [145,146] performed a similar simulation based on a home-made simulation package, which included a detailed 3-layer model of the track. A framework was recently proposed which would investigate train/track/bridge dynamic interactions on HSR [147,148]. Ambrósio et al. studied a high-speed catenary-pantograph [149], showing that other interaction studies are also possible. Escalona et al. [150] reviewed recent research on computer modelling of flexible bodies in railroad vehicle systems, and demonstrated the significant effects on overall vehicle dynamics. In [51], Kouroussis et al. proposed a complete vehicle/track/foundation model using minimal coordinates. In their research, they combined the use of homogeneous

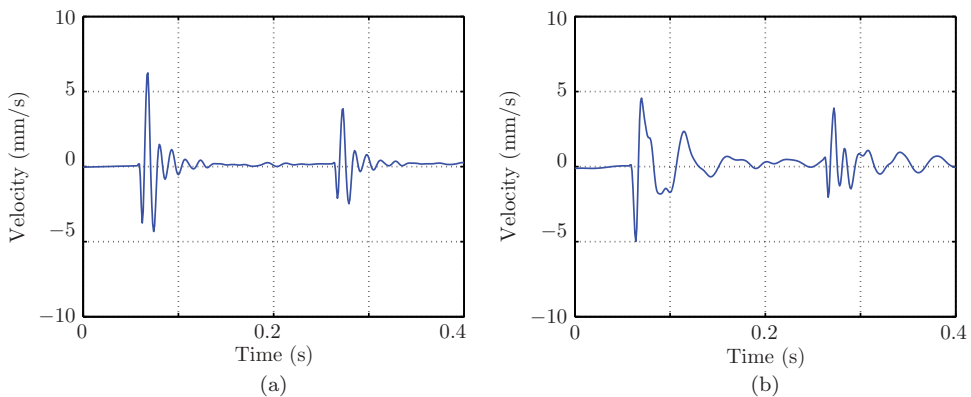


Figure 23. Example of time history of vertical velocity induced by the passing of a bogie on a singular rail surface defect [89]. (a) Using a simple model for the vehicle, (b) Using a multibody model for the vehicle.

transformation matrices for establishing the kinematic relations necessary to build equations of motion. Track vibrations were also calculated from this approach.

In some cases (especially in those of vehicle design and presence of singular rail surface defects), the use of a multibody approach can be beneficial. In [89], Kouroussis et al. demonstrated that the vibrations generated by the passing of a T2000 tram strongly depend on vehicle dynamic characteristics, as illustrated in Figure 23. The effects of a vehicle model composed of unsprung masses are compared, outlining wheels undergoing a static force of loads supplied by a bogie, and the detailed multibody model. Other examples are available in [10,89,151].

8. Concluding remarks

The effect of train vehicle characteristics on railway vibration generation has been investigated through a combination of literature review, numerical analysis, and experimental investigations. A focus was placed on the evolution and suitability of commonly used numerical techniques to investigate the effect of train characteristics. A variety of approaches including constant axle loads, randomly varying axle loads, and multibody loads were appraised and it was found that multibody approaches offered the highest accuracy but required the most computational effort.

Various approaches to modelling track defects were also outlined. It was found that there are a wide range of track quality classification systems available, however it was difficult to make direct comparisons between their accuracy. It was also found that to model vehicle characteristics using non-linear theory, time domain analysis is more suitable, however if the system can be assumed linear then frequency domain analysis is sufficient.

Discussion was also presented to outline the challenge of selecting an appropriate vehicle model that is both accurate and has low computational requirements. Therefore it is recommended that, where possible, the vehicle should be modelled in as much detail as possible.

References

- [1] International Organization for Standardization. ISO 14837-1: mechanical vibration – Ground-borne noise and vibration arising from rail systems – Part 1: General guidance; Geneva: International Organization for Standardization; 2005.
- [2] Degrande G, Schillemans L. Free field vibrations during the passage of a Thalys high-speed train at variable speed. *J Sound Vib.* 2001;247(1):131–144.
- [3] Auersch L, Said S. Attenuation of ground vibrations due to different technical sources. *Earthq Eng Eng Vib.* 2010;9:337–344.
- [4] Madshus C, Kaynia AM. High-speed railway lines on soft ground: dynamic behaviour at critical train speed. *J Sound Vib.* 2000;231(3):689–701.
- [5] Sheng X, Jones CJC, Thompson DJ. A theoretical study on the influence of the track on train-induced ground vibration. *J Sound Vib.* 2004;272(3–5):909–936.
- [6] Galvín P, Domínguez J. Experimental and numerical analyses of vibrations induced by high-speed trains on the Córdoba–Málaga line. *Soil Dyn Earthq Eng.* 2009;29:641–651.
- [7] Costa PA, Calçada R, Cardoso AS. Influence of train dynamic modelling strategy on the prediction of trackground vibrations induced by railway traffic. *Proc IMechE, Part F: J Rail Rapid Transit.* 2012;226(4):434–450.
- [8] Kouroussis G, Verlinden O, Conti C. A two-step time simulation of ground vibrations induced by the railway traffic. *J Mech Eng Sci.* 2012;226(2):454–472.
- [9] Galvín P, François S, Schevenels M, Bongini E, Degrande G, Lombaert G. A 2.5D coupled FE-BE model for the prediction of railway induced vibrations. *Soil Dyn Earthq Eng.* 2010;30(12):1500–1512.

- [10] Kouroussis G, Verlinden O, Conti C. Efficiency of resilient wheels on the alleviation of railway ground vibrations. *Proc IMechE, Part F: J Rail Rapid Transit*. 2012;226(4):381–396.
- [11] Do Rêgo Silva JJ. Acoustic and elastic wave scattering using boundary elements, vol. 18. Southampton: Computational Mechanics Publications; 1994.
- [12] US Department of Transportation (Federal Railroad Administration). High-speed ground transportation. Noise and vibration impact assessment. Technical Report 293630–1, Washington (DC): Office of Railroad Development Washington; 1998.
- [13] Rossi F, Nicolini A. A simple model to predict train-induced vibration: theoretical formulation and experimental validation. *Environ Impact Assess Rev*. 2003;23(3):305–322.
- [14] With C, Bahrekazemi M, Bodare A. Validation of an empirical model for prediction of train-induced ground vibrations. *Soil Dyn Earthq Eng*. 2006;26(11):983–990.
- [15] Verbraken H, Lombaert G, Degrande G. Verification of an empirical prediction method for railway induced vibrations by means of numerical simulations. *J Sound Vib*. 2011;330(8):1692–1703.
- [16] Connolly DP, Kouroussis G, Giannopoulos A, Verlinden O, Woodward PK, Forde MC. Assessment of railway vibrations using an efficient scoping model. *Soil Dyn Earthq Eng*. 2014;58:37–47.
- [17] Krylov VV, Ferguson CC. Calculation of low-frequency ground vibrations from railway trains. *Appl Acoustics*. 1994;42:199–213.
- [18] Krylov VV. Effect of track properties on ground vibrations generated by high-speed trains. *Acustica–Acta Acustica*. 1998;84(1):78–90.
- [19] Kaynia AM, Madshus C, Zackrisson P. Ground vibration from high-speed trains: prediction and countermeasure. *J Geotech Geoenviron Eng*. 2000;126(6):531–537.
- [20] Sheng X, Jones CJC, Petyt M. Ground vibration generated by a load moving along a railway track. *J Sound Vib*. 1999;228(1):129–156.
- [21] Degrande G, Lombaert G. An efficient formulation of Krylov’s prediction model for train induced vibrations based on the dynamic reciprocity theorem. *J Acoust Soc Am*. 2001;110(3):1379–1390.
- [22] Karlström A. An analytical model for ground vibrations from accelerating trains. *J Sound Vib*. 2006;293(3–5):587–598.
- [23] Takemiya H, Bian X. Substructure simulation of inhomogeneous track and layered ground dynamic interaction under train passage. *J Eng Mech*. 2005;131(7):699–711.
- [24] Maldonado M, Chiello O, Houédec DL. Propagation of vibrations due to a tramway line. In: Maeda T, Gautier P-E, Hanson CE, Hemsworth B, Nelson JT, Schulte-Werning B, Thompson D, de Vos P, editors. *Noise and vibration mitigation for rail transportation systems. Proceedings of the 9th International Workshop on Railway Noise*, vol. 99; 2007 Sept 4–8; Berlin. Berlin: SpringerLink; 2008; p. 158–164.
- [25] Lu F, Gao Q, Lin JH, Williams FW. Non-stationary random ground vibration due to loads moving along a railway track. *J Sound Vib*. 2006;298:30–42.
- [26] Sheng X, Jones CJC, Thompson DJ. A theoretical model for ground vibration from trains generated by vertical track irregularities. *J Sound Vib*. 2004;272(3–5):937–965.
- [27] Lombaert G, Degrande G. Ground-borne vibration due to static and dynamic axle loads of InterCity and high-speed trains. *J Sound Vib*. 2009;319:1036–1066.
- [28] Datoussaïd, de Saedeleer B, Verlinden O, Conti C. Vehicle/track interaction and ground propagation of vibrations for urban railway vehicles. *Eur J Mech Environ Eng*. 2000;45(2):87–93.
- [29] Sheng X, Jones CJC, Thompson DJ. A comparison of a theoretical model for quasi-statically and dynamically induced environmental vibration from trains with measurements. *J Sound Vib*. 2003;267(3):621–635.
- [30] Lai CG, Callerio A, Faccioli E, Morelli V, Romani P. Prediction of railway-induced ground vibrations in tunnels. *J Vib Acoustics*. 2005;127(5):503–514.
- [31] Auersch L. The influence of the soil on track dynamics and ground-borne vibration. In: Maeda T, Gautier P-E, Hanson CE, Hemsworth B, Nelson JT, Schulte-Werning B, Thompson D, and de Vos P, editors. *Noise and vibration mitigation for rail transportation systems. Proceedings of the 9th International Workshop on Railway Noise*, vol. 99; 2007 Sept 4–8; Berlin. Berlin: SpringerLink; 2008; p. 122–128.
- [32] Xia H, Cao YM, Roeck GD. Theoretical modeling and characteristic analysis of moving-train induced ground vibrations. *J Sound Vib*. 2010;329(7):819–832.

- [33] Lombaert G, Degrande G, Kogut J, François S. The experimental validation of a numerical model for the prediction of railway induced vibrations. *J Sound Vib.* 2006;297(3–5):512–535.
- [34] Paolucci R, Maffei A, Scandella L, Stupazzini M, Vanini M. Numerical prediction of low-frequency ground vibrations induced by high-speed trains at Ledsgaard, Sweden. *Soil Dyn Earthq Eng.* 2003;23(6):425–433.
- [35] Wang J, Zeng X. Numerical simulations of vibration attenuation of high-speed train foundations with varied trackbed underlayment materials. *J Vib Control.* 2004;10:1123–1136.
- [36] Fujii K, Takei Y, Tsuno K. Propagation properties of train-induced vibrations from tunnels. *Quart Report of RTRI.* 2005;46(3):194–199.
- [37] Yang L, Powrie W, Priest J. Dynamic stress analysis of a ballasted railway track bed during train passage. *J Geotech Geoenviron Eng.* 2009;135(5):680–689.
- [38] Vogiatzis K. Protection of the cultural heritage from underground metro vibration and ground-borne noise in Athens centre: the case of the Kerameikos archaeological museum and Gazi Cultural centre. *Int J Acoustics Vib.* 2012;17:59–72.
- [39] Çelebi E, Kirtel O. Non-linear 2-D FE modeling for prediction of screening performance of thin-walled trench barriers in mitigation of train-induced ground vibrations. *Construct Build Mater.* 2013;42:122–131.
- [40] Yang YB, Hung HH, Chang DW. Train-induced wave propagation in layered soils using finite/infinite element simulation. *Soil Dyn Earthq Eng.* 2003;23:263–278.
- [41] Pakbaz MS, Mehdizadeh R, Vafaeian M, Bagherinia K. Numerical prediction of subway induced vibrations: case study in Iran-Ahwaz City. *J Appl Sci.* 2009;9(11):2001–2015.
- [42] Hall L. Simulations and analyses of train-induced ground vibrations in finite element models. *Soil Dyn Earthq Eng.* 2003;23:403–413.
- [43] Powrie W, Yang LA, Clayton CR. Stress changes in the ground below ballasted railway track during train passage. *Proc IMechE, Part F: J Rail Rapid Transit.* 2007;221(2):247–262.
- [44] Anastasopoulos I, Alfi S, Gazetas G, Bruni S, Leuven AV. Numerical and experimental assessment of advanced concepts to reduce noise and vibration on urban railway turnouts. *J Transport Eng.* 2009;135(5):279–287.
- [45] Stupazzini M, Paolucci R. Ground motion induced by train passage in urban area. In: Sas P, Bergen B, editors. *ISMA2010 International Conference on Noise and Vibration Engineering*; Sept 20–22; Leuven; 2010; p. 3547–3558.
- [46] Gardien W, Stuit HG. Modelling of soil vibrations from railway tunnels. *J Sound Vib.* 2003;267:605–619.
- [47] Ju SH. Finite element investigation of traffic induced vibrations. *J Sound Vib.* 2009;321(3–5):837–853.
- [48] Zhai W, He Z, Song X. Prediction of high-speed train induced ground vibration based on train track-ground system model. *Earthq Eng Vib.* 2010;9(4):545–554.
- [49] Banimahd M, Woodward PK, Kennedy J, Medero GM. Behaviour of train-track interaction in stiffness transitions. *Proc ICE – Transport.* 2011;165(3):205–214.
- [50] Wang J, Jin X, Cao Y. High-speed maglev train-guideway-tunnel-soil modelling of ground vibration. *Proc IMechE, Part F: J Rail Rapid Transit.* 2012;226(3):331–344.
- [51] Kouroussis G, Verlinden O. Prediction of railway induced ground vibration through multi-body and finite element modelling. *Mech Sci.* 2013;4(1):167–183.
- [52] Connolly D, Giannopoulos A, Forde M. Numerical modelling of ground borne vibrations from high speed rail lines on embankments. *Soil Dyn Earthq Eng.* 2013;46:13–19.
- [53] Connolly D, Giannopoulos A, Fan W, Woodward PK, Forde M. Optimising low acoustic impedance back-fill material wave barrier dimensions to shield structures from ground borne high speed rail vibrations. *Construct Build Mater.* 2013;44:557–564.
- [54] El Kacimi A, Woodward PK, Laghrouche O, Medero G. Time domain 3D finite element modelling of train-induced vibration at high speed. *Comput Struct.* 2013;118:66–73.
- [55] Sheng X, Jones CJC, Thompson DJ. Prediction of ground vibration from trains using the wavenumber finite and boundary element methods. *J Sound Vib.* 2006;293(3–5):575–586.
- [56] François S, Schevenels M, Galvín P, Lombaert G, Degrande G. A 2.5D coupled FE-BE methodology for the dynamic interaction between longitudinally invariant structures and a layered halfspace. *Comput Methods Appl Mech Eng.* 2010;199:1536–1548.
- [57] Costa PA, Calada R, Cardoso AS, Bodare A. Influence of soil non-linearity on the dynamic response of high-speed railway tracks. *Soil Dyn Earthq Eng.* 2010;30(4):221–235.

- [58] Gao GY, Chen QS, He JF, Liu F. Investigation of ground vibration due to trains moving on saturated multi-layered ground by 2.5D finite element method. *Soil Dyn Earthq Eng.* 2012;40:87–98.
- [59] O'Brien J, Rizos DC. A 3D BEM-FEM methodology for simulation of high speed train induced vibrations. *Soil Dyn Earthq Eng.* 2005;25(4):289–301.
- [60] Andersen L, Jones CJC. Coupled boundary and finite element analysis of vibration from railway tunnels – comparison of two- and three-dimensional models. *J Sound Vib.* 2006;293(3–5):611–625.
- [61] Auersch L. Dynamic axle loads on tracks with and without ballast mats: numerical results of three-dimensional vehicle-track-soil models. *Proc IMechE, Part F: J Rail Rapid Transit.* 2006;220(2):169–183.
- [62] Chebli H, Clouteau D, Schmitt L. Dynamic response of high-speed ballasted railway tracks: 3D periodic model and in situ measurements. *Soil Dyn Earthq Eng.* 2008;28(2):118–131.
- [63] Galvín P, Romero A, Domínguez J. Fully three-dimensional analysis of high-speed train-track-soil-structure dynamic interaction. *J Sound Vib.* 2010;329(24):5147–5163.
- [64] Romero A, Galvín P, Domínguez J. Fully 3D analysis of HST-track-soil-structure dynamic interaction. In: Sas P, Bergen B, editors. *ISMA2010 International Conference on Noise and Vibration Engineering*; Sept 20–22; Leuven; 2010; p. 3531–3546.
- [65] Thornely-Taylor R. The prediction of vibration, groundborne and structure-radiated noise from railways using finite difference methods – Part I – Theory. *Proc Inst Acoust*;2004;26:1–11.
- [66] Hussein MFM, Hunt HEM. A numerical model for calculating vibration due to a harmonic moving load on a floating-slab track with discontinuous slabs in an underground railway tunnel. *J Sound Vib.* 2009;321(1–2):363–374.
- [67] Jones S, Hunt H. Effect of inclined soil layers on surface vibration from underground railways using the thin-layer method. *ASCE J Eng Mech.* 2011;137(12):887–900.
- [68] Esveld C. *Modern railway track*. 2nd ed. Zaltbommel: MRT Production; 2001.
- [69] Iwnicki S. *Handbook of railway vehicle dynamics*. New York (NY): CRC Press; 2006.
- [70] Thompson DJ. *Railway noise and vibration: mechanisms, modelling and means control*. Oxford: Elsevier; 2009.
- [71] Xia H, Calada R, editors. *Traffic induced environmental vibrations and controls: theory and application*. New York (NY): Nova Science Publishers; 2013.
- [72] Suda Y, Michitsuji Y, Sugiyama H. Next generation unconventional trucks and wheel-rail interfaces for railways. *Int J Railway Technol.* 2012;1(1):1–29.
- [73] Wilson GP, Saurenman HJ, Nelson JT. Control of ground-borne noise and vibration. *J Sound Vib.* 1983;87(2):339–350.
- [74] Nelson JT. Recent developments in ground-borne noise and vibration control. *J Sound Vib.* 1996;193(1):367–376.
- [75] Alias J. *La voie ferrée – technique de construction et d'entretien*. 2nd ed. Paris: Eyrolles; 1984.
- [76] Heckl M, Hauck G, Wettschureck R. Structure-borne sound and vibration from rail traffic. *J Sound Vib.* 1996;193(1):175–184.
- [77] Dahlberg T. *Railway track dynamics – a survey*. Technical Report Railtrdy.doc/2003-11-06/td. Linkping: Linkping University; 2003.
- [78] Kouroussis G, Verlinden O, Conti C. Influence of some vehicle and track parameters on the environmental vibrations induced by railway traffic. *Vehicle Syst Dyn.* 2012;50(4):619–639.
- [79] Kouroussis G, Conti C, Verlinden O. Investigating the influence of soil properties on railway traffic vibration using a numerical model. *Vehicle Syst Dyn.* 2013;51(3):421–442.
- [80] Kouroussis G, Connolly DP, Forde MC, Verlinden O. Train speed calculation using ground vibrations. *Proc IMechE, Part F: J Rail Rapid Transit.* doi:10.1177/0954409713515649.
- [81] Connolly DP, Kouroussis G, Fan W, Percival M, Giannopoulos A, Woodward P, Verlinden O, Forde MC. An experimental analysis of embankment vibrations due to high speed rail. Paper presented at: 12th International Railway Engineering Conference; Jul 10–11. London: Railway Engineering; 2013.
- [82] Kouroussis G, Connolly D, Forde M, Verlinden O. An experimental study of embankment conditions on high-speed railway ground vibrations. Paper presented at: 20th International Congress on Sound and Vibration, ICSV20; Jul 7–11; Bangkok; 2013.

- [83] Dieterman HA, Metrikine AV. The equivalent stiffness of a half-space interacting with a beam. Critical velocities of a moving load along the beam. *Eur J Mech A/Solids*. 1996;15(1):67–90.
- [84] Takemiya H. Simulation of track-ground vibrations due to a high-speed train: the case of X-2000 at Ledsgard. *J Sound Vib*. 2003;261(3):503–526.
- [85] Lefeuvre-Mesgouez G, Peplow AT, Houédec DL. Surface vibration due to a sequence of high speed moving harmonic rectangular loads. *Soil Dyn Earthq Eng*. 2002;22(6):459–473.
- [86] Banimahd M. Advanced finite element modelling of coupled train-track systems: a geotechnical perspective [Ph.d. dissertation]. Edinburgh: Heriot Watt University, School of Built Environment; 2008.
- [87] Degrande G, Chatterjee P, Jacobs S, Charlier J, Bouvet P, Brassens D. CONVURT Project experimental results of free field and structural vibrations due to underground railway traffic. Paper presented at: 6th World Congress on Railway Research; Sept 28–Oct 1; Edinburgh; 2003.
- [88] Vogiatzis C, Chaikali S. Vibration and ground borne noise criteria and mitigation measures at Athens tramway. Paper presented at: 11th International Congress on Sound and Vibration; Jul 5–8; St. Petersburg; 2004.
- [89] Kouroussis G, Verlinden O, Conti C. On the interest of integrating vehicle dynamics for the ground propagation of vibrations: the case of urban railway traffic. *Vehicle Syst Dyn*. 2010;48(12):1553–1571.
- [90] Kouroussis G, Verlinden O, Conti C. Contribution of vehicle/track dynamics to the ground vibrations induced by the Brussels tramway. In: Sas P, Bergen B, editors. ISMA2010 International Conference on Noise and Vibration Engineering; Sept 20–22; Leuven. Leuven: ISMA; 2010; p. 3489–3502.
- [91] Ewing WM, Jardetzky WS, Press F. Elastic waves in layered media. New York (NY): McGraw-Hill Book Company; 1957.
- [92] Gutowski TG, Dym CL. Propagation of ground vibrations: a review. *J Sound Vib*. 1976;49:179–193.
- [93] Miller GF, Pursey H. On the partition of energy between elastic waves in a semi-infinite solid. *Proc Royal Soc (London)*. 1955;233:55–69.
- [94] Ditzel A, Herman GC, Drijkoningen GG. Seismograms of moving trains: a comparison of theory and measurements. *J Sound Vib*. 2001;248(4):635–652.
- [95] Jones DV, Petyt M. Ground vibration in the vicinity of a strip load: an elastic layer on a rigid foundation. *J Sound Vib*. 1992;152(3):501–515.
- [96] Triepaischajonsak N, Thompson DJ, Jones CJC, Ryue J, Priest JA. Ground vibration from trains: experimental parameter characterization and validation of a numerical model. *Proc IMechE, Part F: J Rail Rapid Transit*. 2011;225(2):140–153.
- [97] Grassie SL, Gregory RW, Harrison D, Johnson KL. The dynamic response of railway track to high frequency vertical excitation. *J Mech Eng Sci*. 1982;24(2):77–90.
- [98] Knothe K, Grassie SL. Modelling of railway track and vehicle/track interaction at high frequencies. *Vehicle Syst Dyn*. 1993;22:209–262.
- [99] Zhai W, Sun X. A detailed model for investigating vertical interaction between railway vehicle and track. *Vehicle Syst Dyn*. 1994;23(Suppl):603–615.
- [100] Ahlbeck DR, Meacham HC, Prause RH. The development of analytical models for railroad track dynamics. In: Kerr A, editor. *Proceedings of Symposium on Railroad Track Mechanics*; Apr 21–23; Princeton, NJ. Oxford; 1975; p. 239–263.
- [101] Suiker ASJ. The mechanical behaviour of ballasted railway tracks [Ph.d. dissertation]. Delft: Delft Technical University; 2002.
- [102] Auersch L. Dynamic plate-soil interaction – finite and infinite, flexible and rigid plates on homogeneous, layered or Winkler soil. *Soil Dyn Earthq Eng*. 1996;15(1):51–59.
- [103] Vostroukhov AV, Metrikine AV. Periodically supported beam on a visco-elastic layer as a model for dynamic analysis of a high-speed railway track. *Int J Solids Struct*. 2003;40(21):5723–5752.
- [104] Knothe K, Wu Y. Receptance behaviour of railway track and subgrade. *Arch Appl Mech*. 1998;68:457–470.
- [105] Kouroussis G, Gazetas G, Anastasopoulos I, Conti C, Verlinden O. Discrete modelling of vertical track–soil coupling for vehicle–track dynamics. *Soil Dyn Earthq Eng*. 2011;31(12):1711–1723.

- [106] Virieux J. P-SV wave propagation in heterogeneous media: velocity-stress finite-difference method. *Geophysics*. 1986;51:889–901.
- [107] Graves RW. Simulating seismic wave propagation in 3D elastic media using staggered-grid finite differences. *Bull Seismol Soc Am*. 1091–1106;86 (4):983–990.
- [108] Katou M, Matsuoka T, Yoshioka O, Sanada Y, Miyoshi T. Numerical simulation study of ground vibrations using forces from wheels of a running high-speed train. *J Sound Vib*. 2008;318(4–5):830–849.
- [109] Smith IM, Griffiths DV. *Programming the finite element method*. 2nd ed. Essex: John Wiley & Sons; 1988.
- [110] Petyt M. *Introduction to finite element vibration analysis*. New York (NY): Cambridge University Press; 2010.
- [111] Liu G, Quek S. *The finite element method: a practical course*. Oxford: Butterworth–Heinemann; 2003.
- [112] Banerjee PK, Butterfield R. *Boundary element methods in engineering science*. London: McGraw-Hill Book Company; 1981.
- [113] Dominguez J. *Boundary elements in dynamics*. Southampton: Computational Mechanics Publications; 1993.
- [114] Hall WS. *The boundary element method*. Dordrecht: Kluwer Academic Publishers; 1994.
- [115] Song C, Wolf JP. The scaled boundary finite-element method – alias consistent infinitesimal finite element cell method – or elastodynamics. *Comp Methods Appl Mech Eng*. 1997;147 (3–4):329–355.
- [116] Ekevid T, Wiberg NE. Wave propagation related to high-speed train: a scaled boundary FE approach for unbounded domains. *Comput Methods Appl Mech Eng*. 2002;191(36):3947–3964.
- [117] Kausel E. Thin-layer method: formulation in the time domain. *Int J Numerical Methods Eng*. 1994;37(6):927–941.
- [118] Auersch L. Ground vibration due to railway traffic – the calculation of the effects of moving static loads and their experimental verification. *J Sound Vib*. 2006;293(3–5):599–610.
- [119] Ju SH, Lin HT, Huang JY. Dominant frequencies of train-induced vibrations. *J Sound Vib*. 2009;319(1–2):247–259.
- [120] Ni SH, Huang YH, Lo KF. An automatic procedure for train speed evaluation by the dominant frequency method. *Comput Geotech*. 2011;38(4):416–422.
- [121] Krylov VV. Spectra of low-frequency ground vibrations generated by high-speed trains on layered ground. *J Low Freq Noise Vib Active Control*. 1997;16(4):257–270.
- [122] Garg VK, Dukkipati RV. *Dynamics of railway vehicle systems*. Toronto (ON): Academic Press; 1984.
- [123] InTec GmbH. *SIMPACT Theory Manual (release 8.6)*. Gilching; 2006.
- [124] Andersson E, Berg M, Stichel S. *Rail Vehicle Dynamics (In Swedish: Sprfordons dynamik)*. Stockholm: KTH Jrmvgsteknik; 2000.
- [125] International Organization for Standardization. *ISO 8608: mechanical vibration – road surface profiles – Reporting of measured data*; 1995.
- [126] Braun H, Hellenbroich T. *Messergebnisse von strassenunebenheiten*. VDI Berichte. 1991;877:47–80.
- [127] Kouroussis G, Van Parys L, Conti C, Verlinden O. Prediction of ground vibrations induced by urban railway traffic: an analysis of the coupling assumptions between vehicle, track, soil, and buildings. *Int J Acoustics Vib*. 2013;18(4):163–172.
- [128] Auersch L. Theoretical and experimental excitation force spectra for railway-induced ground vibration: vehicle–track–soil interaction, irregularities and soil measurements. *Vehicle Syst Dyn*. 2010;48(2):235–261.
- [129] Johansson A, Nielsen JCO. Out-of-round railway wheels – wheel-rail contact forces and track response derived from field tests and numerical simulations. *Proc IMechE, Part F: J Rail Rapid Transit*. 2003;217(2):135–146.
- [130] Nielsen JCO. Numerical prediction of rail roughness growth on tangent railway tracks. *J Sound Vib*. 2003;267(3):537–548.
- [131] Dings PC, Dittich MG. Roughness on Dutch railway wheels and rails. *J Sound Vib*. 1996;193(1):103–112.
- [132] Hiensch M, Nielsen JCO, Verheijen E. Rail corrugation in The Netherlands – measurements and simulations. *Wear*. 2002;253(1–2):140–149.

- [133] Barke DW, ChiuWK. A review of the effects of out-of-round wheels on track and vehicle components. Proc IMechE, Part F: J Rail Rapid Transit. 2012;219:151–175.
- [134] Verheijen E. A survey on roughness measurements. J Sound Vib. 2006;293(3–5):784–794.
- [135] Kalker JJ. Three-dimensional elastic bodies in rolling contact. Dordrecht: Kluwer Academic; 1990.
- [136] International Organization for Standardization. ISO 2631-2: mechanical vibration and shock – evaluation of human exposure to whole-body vibration – Part 2: Vibration in buildings (1 Hz to 80 Hz); 2003.
- [137] Deutsches Institut für Normung. DIN 4150-2: Structural vibrations – Part 2: Human exposure to vibration in buildings. 1999.
- [138] Deutsches Institut für Normung. DIN 4150-3: Structural vibrations – Part 3: Effects of vibration on structures. 1999.
- [139] Costa PA, Calada R, Cardoso AS. Vibrations induced by railway traffic: influence of the mechanical properties of the train on the dynamic excitation mechanism. In: Roeck GD, Degrande G, Lombaert G, Müller G. Leuven, editors. 8th International Conference on Structural Dynamics: EURODYN 2011; Jul 4–6; Leuven. Leuven; 2011; p. 804–811.
- [140] Mirza AA, Frid A, Nielsen JCO, Jones CJC. Ground vibration induced by railway traffic – the influence of vehicle parameters. In: Maeda T, Gautier P-E, Hanson CE, Hemsworth B, Nelson JT, Schulte-Werning B, Thompson D, de Vos P, editors. Noise and Vibration Mitigation for Rail Transportation Systems. Proceedings of the 10th International Workshop on Railway Noise, vol. 118; 2010 Oct 18–22. Nagahama: SpringerLink; 2012; p. 259–266.
- [141] Alexandrou G, Kouroussis G, Verlinden O. Modelling the effect of wheel flat on railway-induced ground vibrations. In: Pombo J, editor. Proceedings of the Second International Conference on Railway Technology: Research, Development and Maintenance. Ajaccio: Civil-Comp Press; 2014.
- [142] Popp K, Schiehlen W. Ground vehicle dynamics. Berlin: Springer. 2010.
- [143] Iwnicki S. Manchester benchmarks for rail vehicle simulation. Vehicle Syst Dyn. 1998;30(3–4):295–313.
- [144] Dietz S, Hippmann G, Schupp G. Interaction of vehicles and flexible tracks by co-simulation of multibody vehicle systems and finite element track models. Vehicle Syst Dyn Suppl (Dyn Vehicles Roads Tracks). 2002;37:372–384.
- [145] Zhai WM, True H. Vehicle-track dynamics on a ramp and on the bridge: simulation and measurements. Vehicle Syst Dyn. 1999;33(Suppl):604–615.
- [146] Zhai W, Wang K, Cai C. Fundamentals of vehicle–track coupled dynamics. Vehicle Syst Dyn. 2009;47(11):1349–1376.
- [147] Zhai W, Xia H, Cai C, Gao M, Li X, Guo X, Zhang N, Wang K. High-speed train–track–bridge dynamic interactions – Part I: theoretical model and numerical simulation. Int J Rail Transport. 2013;1(1–2):3–24.
- [148] Zhai W, Wang S, Zhang N, Gao M, Xia H, Cai C, Zhao C. High-speed train–track–bridge dynamic interactions – Part II: experimental validation and engineering application. Int J Rail Transport. 2013;1(1–2):25–41.
- [149] Ambrósio J, Pombo J, Rauter F, Pereira M. A memory based communication in the co-simulation of multibody and finite element codes for pantograph-catenary interaction simulation. In: Bottasso CL, editor. Multibody Dynamics, vol. 12 of Computational Methods in Applied Sciences. Berlin: Springer; 2008. p. 231–252.
- [150] Escalona JL, Sugiyama H, Shabana AA. Modelling of structural flexibility in multibody railroad vehicle systems. Vehicle Syst Dyn. 2013;51(7):1027–1058.
- [151] Kouroussis G, Pauwels N, Brux P, Conti C, Verlinden O. A numerical analysis of the influence of tram characteristics and rail profile on railway traffic ground-borne noise and vibration in the Brussels Region. Sci Total Environ. doi:10.1016/j.scitotenv.2013.05.083.
- [152] Kouroussis G, Conti C, Verlinden O. Experimental study of ground vibrations induced by Brussels IC/IR trains in their neighbourhood. Mech Indus. 2013;14(02):99–105.
- [153] Kouroussis G, Verlinden O, Conti C. Free field vibrations caused by high-speed lines: measurement and time domain simulation. Soil Dyn Earthq Eng. 2011;31(4):692–707.
- [154] Auersch L. The excitation of ground vibration by rail traffic: theory of vehicle-track-soil interaction and measurements on high-speed lines. J Sound Vib. 2005;284(1–2):103–132.

Appendix Geometrical and dynamic characteristics of a variety of rolling stocks

This appendix provides an overview of some of the most commonly found rail vehicles and approximations for their vehicle properties. The list is not exhaustive but focuses on the vehicles most frequently found in vibration related literature. It is ordered by typical operating vehicle speed. For researchers who want to analyse the dynamic effects of vehicles in urban environments, one challenge is obtaining the dynamic parameters required for vehicle modelling. This section provides detailed tables with these values.

For light transit vehicles (trams), only the low-floor, T2000 tram designed by Bombardier transport, and found operating in Brussels has been detailed. It has double ended cars with a driver's cabin on both ends which is separated from the passengers. Figure A1 presents the key dimensions, complimented by the dynamic characteristic in Table A1. This particular design imposes a complex articulated structure allowing each wheel to remain tangential to the rail. Additionally, the bogies have independent wheels inside which the motors are mounted. These wheels are also equipped with resilient rubber, thus increasing the unsprung masses of the vehicle. This particular configuration can induce large ground vibrations compared to other trams with similar axle loading. These effects have been studied extensively in [10,89,127].

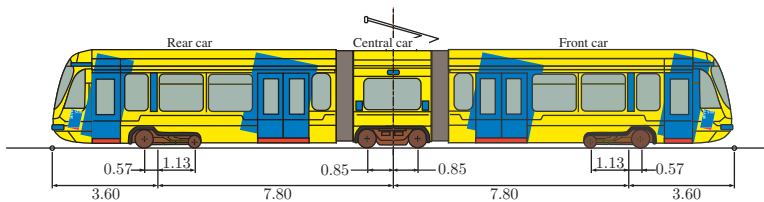


Figure A1. Configuration of the T2000 tram.

Table A1. T2000 tram dynamic properties (issued from [89]).

	m_c (kg)	m_b (kg)	I_b (kg.m ²)	m_w (kg)
Front and rear cars	7580	1800	300	1025 (160)
Central car	2600	1800	300	1025
	k_i (MN/m)		d_i (kNs/m)	
Primary suspension ($i = 1$)	44 (5.88)		18 (6)	
Secondary suspension ($i = 2$)	960		56.25	

Note: Under parentheses, values for the trailer wheels.

The AM96 unit, largely used by the Belgian Railway Operator SNCB, is the most recent developed train, and is commonly used for long distance routes. It is typically used for InterCity and InterRegion connections, due to its excellent passenger comfort. It uses the latest bogie technology developed in the high-speed rail sector, in order to obtain a smoother ride, with a maximum speed of 160 km/h. It consists of three self-propelled carriages, designated by HVBX, HVB, and HVADX. The leading wagon HVBX is equipped with motorized bogies, with the HVB (at middle) and HVADX (at end) being trailer carriages. Figure A2 presents the configurations and main dimensions, complimented by the dynamic and geometrical information provided in Table A2. The impact of this train on urban environments was studied in [152]. An alternative Belgian InterCity train is the I11 passenger car, as studied by Lombaert et al. [27]. It can operate in push-pull mode with a class HLE 13 locomotive and a maximum speed of 200 km/h. The units have also been used with two driving trailers and a mid-train locomotive. Its design is also based on HST technology, with secondary air suspension to improve passenger comfort. It consists on three car types: the end coaches HVI1BDx

and HVI11B, and a central coach HVI11A similar to the HVI11B type. Geometric and dynamic data are provided in Figure A3 and Table A3.

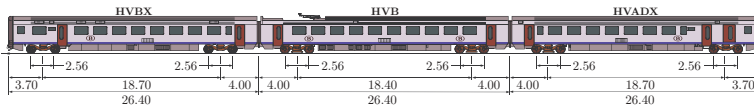


Figure A2. Configuration of the AM96 electric multiple unit.

Table A2. AM96 unit dynamic properties.

	m_c (kg)	I_c (kg.m ²)	m_b (kg)	I_b (kg.m ²)	m_w (kg)
HVB car	25200	1.26×10^6	6900	1.52×10^3	1700
HVADX car	28900	1.45×10^6	7050	1.58×10^3	1700
HVBX car	25930	1.30×10^6	11800	2.60×10^3	1700
	k_1 (MN/m)	d_1 (kNs/m)	k_2 (MN/m)	d_2 (kNs/m)	
HVB car	1.30	3.7	0.69	22.6	
HVADX car	1.30	3.7	0.69	22.6	
HVBX car	1.81	1.14	0.69	14	

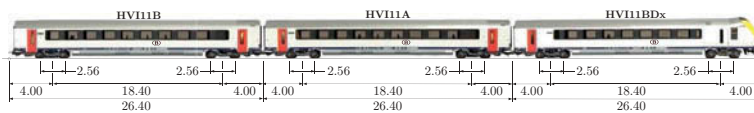


Figure A3. Configuration of the I11 multiple unit.

Table A3. I11 unit dynamic properties.

	m_c (kg)	I_c (kg.m ²)	m_b (kg)	I_b (kg.m ²)	m_w (kg)
HVI11A	26840	1.35×10^6	13600	2.95×10^3	1500
HVI11B	26808	1.35×10^6	13600	2.95×10^3	1500
HVI11BDx	27544	1.38×10^6	13600	2.95×10^3	1544
	k_1 (MN/m)	d_1 (kNs/m)	k_2 (MN/m)	d_2 (kNs/m)	
HVI11A	0.95	7.5	0.24	22.6	
HVI11B	0.95	7.5	0.24	22.6	
HVI11BDx	0.95	7.5	0.24	22.6	

HST is the most commonly studied train type in ground vibration research. In Europe, the well-known TGV family of HSTs was built by Alstom, Siemens, and/or Bombardier. Details of previous research into various HSTs types are as follows:

- Thalys (Figure A4 – Table A4) – was studied extensively in [2,52,153].
- TGV Atlantique and TGV réseau – have similar properties (Figure A4 – Table A5) and have been studied in [9] and partially in [81,82].

- Eurostar HST (Figure A5 – Table A6) – presenting a particular configuration in the middle inherent to the channel tunnel configuration (presence of two side carriages added for safety reasons) and studied in [153].
- The German Intercity-Express (ICE) – similar to the TGV (Figure A6 – Table A7), but with various generations; it was studied in [118,154].
- The Alta Velocidad Espanola (AVE) S-100 – used in Spain (Figure A4 – Table A8) and analysed by Galvin et al. [63].

Each HST type detailed above has a similar configuration, in which the two locomotives are supported by two bogies. Instead of the conventional bogie configuration of two-to-a-car, the carriage bogies are placed half under one car and half under the next (Jacobs' bogies). The only exception is that of the side carriage bogies near the power car and at the middle of the vehicle. Other notable conventional HSTs include:

- The Alfa Pendular HST with tilting technology (Figure A7 – Table A9) – rides in Portugal and studied by Costa et al. [7].
- The Swedish X-2000 HST (Figure A8) – first analysed by Kaynia et al. [19] and one of the earliest trains to be associated with supercritical Rayleigh wave phenomenon.

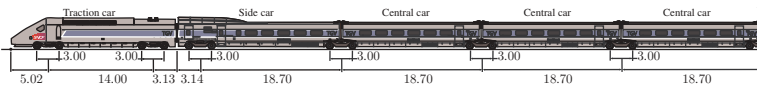


Figure A4. French TGV dimensions (similar configuration for Thalys and AVE S-100 HSTs).

Table A4. Thalys HST dynamic properties (issued from [153]).

	m_c (kg)	I_c (kg.m ²)	m_b (kg)	I_b (kg.m ²)	m_w (kg)
Traction cars	53442	1.15×10^6	3261	2.87×10^3	2009
Side cars	34676	1.49×10^3	8156	7.19×10^3	2009
Central cars	14250	0.61×10^3	1400	1.23×10^3	2050
	k_1 (MN/m)	d_1 (kNs/m)	k_2 (MN/m)	d_2 (kNs/m)	
Traction cars	2.09	40	2.45	40	
Side cars	2.09	40	2.45	40	
Central cars	1.63	40	0.93	40	

Table A5. TGV Atlantique dynamic properties (issued from [9]).

	m_c (kg)	I_c (kg.m ²)	m_b (kg)	I_b (kg.m ²)	m_w (kg)
Traction cars	55790	1.15×10^6	2380	1.48×10^3	2048
Side cars	24000	1.48×10^3	3040	2.68×10^3	2003
Central cars	24000	1.48×10^3	3040	2.68×10^3	2003
	k_1 (MN/m)	d_1 (kNs/m)	k_2 (MN/m)	d_2 (kNs/m)	
Traction cars	2.45	20	2.45	40	
Side cars	1.40	10	0.82	40	
Central cars	1.40	10	0.82	48	

Additional HSTs that are interesting due to their configurations are: the Spanish AVE Class 103 HST (Figure A6) and the British Class 365 Javelin HST (Figure A9) with conventional bogies, and the tilting Spanish Talgo 250 with independent wheels (Figure A10) and dual-gauge system.

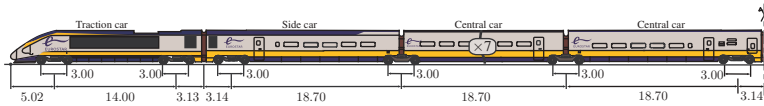


Figure A5. Eurostar HST dimensions.

Table A6. Eurostar HST dynamic properties.

	m_c (kg)	I_c (kg.m ²)	m_b (kg)	I_b (kg.m ²)	m_w (kg)
Traction cars	54166	1.12×10^6	3075	1.92×10^3	2046
Side cars	33854	2.09×10^3	9440	8.16×10^3	2046
Central cars	27083	1.67×10^3	2360	2.04×10^3	2046
	k_1 (MN/m)	d_1 (kNs/m)	k_2 (MN/m)	d_2 (kNs/m)	
Traction cars	2.63	12	3.26	90	
Side cars	2.20	12	0.91	2	
Central cars	2.07	12	0.61	4	

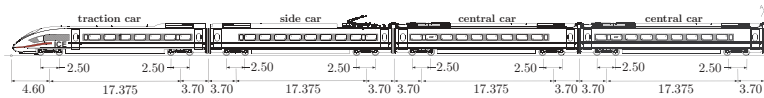


Figure A6. ICE train dimensions (similar configuration for AVE Class 103 HST).

Table A7. ICE train dynamic properties.

	m_c (kg)	I_c (kg.m ²)	m_b (kg)	I_b (kg.m ²)	m_w (kg)
Traction cars	50000	1.03×10^6	5154	3.22×10^3	1600
Central cars	35000	2.16×10^3	2840	2.46×10^3	1750
	k_1 (MN/m)	d_1 (kNs/m)	k_2 (MN/m)	d_2 (kNs/m)	
Traction cars	4.30	24	1.43	70	
Central cars	1.40	120	0.45	40	

Table A8. AVE S-100 HST dynamic properties (issued from [63]).

	m_c (kg)	I_c (kg.m ²)	m_b (kg)	I_b (kg.m ²)	m_w (kg)
Traction cars	55790	1.15×10^6	2380	1.48×10^3	2048
Side cars	24000	1.48×10^3	3040	2.68×10^3	2003
Central cars	26950	1.66×10^3	3040	2.68×10^3	2003
	k_1 (MN/m)	d_1 (kNs/m)	k_2 (MN/m)	d_2 (kNs/m)	
Traction cars	1.20	10	2.45	40	
Side cars	0.70	5	0.82	48	
Central cars	0.70	5	0.82	48	

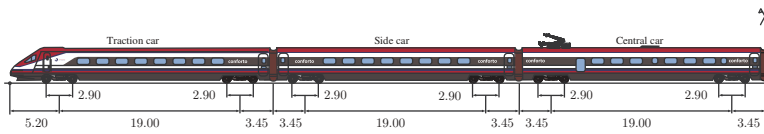


Figure A7. Alfa Pendular HST dimensions.

Table A9. Alfa Pendular HST dynamic properties (issued from [7]).

	m_c (kg)	I_c (kg.m ²)	m_b (kg)	I_b (kg.m ²)	m_w (kg)
Traction cars	32901 33201	2.08×10^6	4932	5.15×10^3	1538
Side cars	32910 35701	2.08×10^3	4823	5.09×10^3	1538
Central cars	33124 33524	2.08×10^3	4712	5.00×10^3	1538
	k_1 (MN/m)	d_1 (kNs/m)	k_2 (MN/m)	d_2 (kNs/m)	
Traction cars	3.42	36	1.32	36	
Side cars	3.42	36	1.32	36	
Central cars	3.42	36	1.32	36	

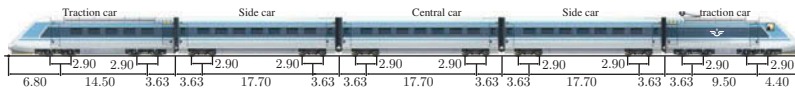


Figure A8. X-2000 HST dimensions.

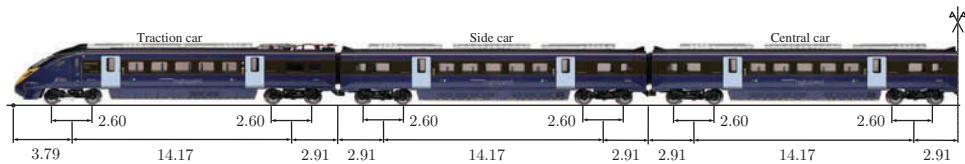


Figure A9. Javelin 395 HST dimensions.

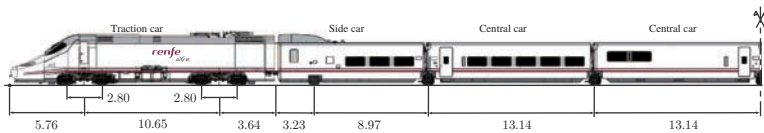


Figure A10. Talgo 250 HST dimensions.